Am J Cancer Res 2025;15(7):3164-3187
www.ajcr.us /ISSN:2156-6976/ajcr0156127

Original Article

FOXK1-induced upregulation of NXPH4 predicts poor prognosis and promotes hepatocellular carcinoma progression via PI3K/Akt pathway

Yafeng Wang*, Zhongqiu Li*, Liancai Wang*, Yongnian Ren, Deyu Li

*Department of Hepato-Biliary Pancreatic Surgery, Henan Provincial People's Hospital, Zhengzhou, Henan, China. *Equal contributors.*

Received February 26, 2024; Accepted June 6, 2025; Epub July 15, 2025; Published July 30, 2025

Abstract: Hepatocellular carcinoma (HCC) stands out as a remarkably diverse and complex disease, presenting a myriad of challenges when it comes to predicting prognostic outcomes. Although lactate and branched-chain amino acids (BCAA) are important for the development and progression of various tumors, their function in HCC progression remained largely unclear. The study aimed to identify molecular subtypes in HCC based on lactate metabolism and BCAA metabolism. Clustering 370 HCC patients revealed two distinctive subtypes associated with unfavorable prognosis. Differential expression analysis identified 941 DEGs in lactate metabolism subtypes and 518 in BCAA metabolism subtypes, primarily linked to tumor and metabolism pathways. Prognostic analysis identified 27 LRG-BCAA-DGEs inversely correlated with long-term survival across various cancers. Methylation analysis showed a negative correlation between methylation and mRNA expression of these genes, with limited impact on survival outcomes. NXPH4, dysregulated across tumors, exhibited complex associations with immune cells and prognostic implications in HCC. Functional analysis revealed DEGs associated with endodermal cell differentiation and metabolic pathways. NXPH4 knockdown suppressed HCC cell proliferation, migration, and invasion, indicating its potential as a therapeutic target. Additionally, NXPH4 modulated glucose metabolism via the PI3K/Akt pathway. FOXK1 was identified as a potential transcriptional regulator of NXPH4, suggesting a regulatory axis in HCC tumorigenesis. The study highlights the molecular complexity of HCC, providing insights into potential biomarkers and therapeutic targets.

Keywords: Hepatocellular carcinoma, branched-chain amino acids, lactate, prognosis, PI3K/Akt pathway, NXPH4

Introduction

Liver cancer, a deadly ailment with a high incidence and poor prognosis, is predominantly represented by liver hepatocellular carcinoma (HCC), constituting 75%-85% of cases within the spectrum of liver malignancies [1, 2]. As a prevalent cancer, numerous factors have been substantiated as contributors to its onset, encompassing viral infections and the presence of cirrhosis. Liver cancer shows significant regional variations globally [3, 4]. Some regions, such as East Asia (particularly China), Southeast Asia, and sub-Saharan Africa, have relatively higher incidence rates of liver cancer. Factors like diet, prevalence of viral hepatitis infections, and other environmental factors in these areas may be associated with the occurrence of liver cancer [5, 6]. The risk of liver cancer increases with age, particularly in the age group of 60 and above. Long-term chronic liver diseases, liver cirrhosis, and other factors contribute to an elevated risk of liver cancer in the elderly population [7]. Although some patients with HCC undergo radical hepatectomy, the high occurrence of postoperative recurrence and metastasis remains a significant challenge for patient survival. Therefore, the exploration of reliable and promising prognostic indicators for individuals with HCC is of paramount importance.

Lactate is an organic acid and one of the metabolic byproducts in the process of lactate fermentation. It is produced by microorganisms such as lactic acid bacteria under anaerobic conditions [8, 9]. Lactate is generated as part of the metabolic pathway during the breakdown

https://doi.org/10.62347/ZLOS1416

of sugars. Under anaerobic conditions, sugars like glucose are converted into lactate through the process of glycolysis [10]. This phenomenon occurs in various cells, including microorganisms and muscle cells. Tumor cells often exhibit enhanced glycolysis, producing lactate even in the presence of oxygen, a phenomenon known as the "Warburg Effect". Due to the imperfect vascular structure in tumor tissues, a hypoxic environment further contributes to the accumulation of lactate [11, 12]. The accumulation of lactate can impact the survival, proliferation, and metastasis of tumor cells. On one hand, lactate can influence the acid-base balance in the tumor microenvironment, leading to acidification and promoting tumor invasion and metastasis. On the other hand, lactate may also play a role in signaling and regulating cellular behaviors within tumor cells [13-15]. The accumulation of lactate may affect the function of immune cells, influencing the immune escape of tumors. Some studies suggest that high lactate concentrations can impact the activity of immune cells, suppressing their cytotoxic effects and favoring the evasion of immune surveillance by tumors [16, 17]. Nevertheless, it is still not known how lactate relates to HCC.

Branched Chain Amino Acids (BCAAs) constitute a class of amino acids, including Isoleucine, Valine and Leucine. They are termed branched-chain due to the presence of a branched chemical structure [18]. These amino acids are essential, meaning the body cannot synthesize them and must obtain them through dietary sources. Leucine activates the mTOR signaling pathway within cells, a critical pathway associated with protein synthesis and cell growth [19, 20]. Certain cancer cells exhibit a heightened dependence on BCAAs, particularly Leucine, which may be linked to their increased requirements for growth and proliferation. Valine and Isoleucine participate in the degradation of muscle proteins, releasing amino acids as a source of energy [21, 22]. In specific scenarios, tumor cells may utilize BCAAs from surrounding normal tissues as an energy source, leading to adverse effects on the body. Leucine, by activating the mTOR pathway, promotes protein synthesis, potentially playing a role in the growth and proliferation of tumor cells [23, 24]. Some studies suggest that modulating the metabolism of BCAAs could influence the biological behavior of tumor cells. In summary, branched-chain amino acids play crucial roles in cellular metabolism, and their relationship with tumor cells involves influencing pathways related to growth, energy metabolism, and protein synthesis. Gaining a better grasp of this connection can help shed light on the underlying biology of cancer cells and lead to the identification of new therapeutic targets. Unfortunately, research on the link between BCAAs and HCC is lacking at the moment.

Our research findings demonstrate that the combined expression of lactate and BCAAs metabolism genes serves as a reliable indicator for the prognosis of HCC, offering valuable guidance for treatment decisions. Through consensus clustering, 370 samples were categorized into high and low-risk groups. Kaplan-Meier survival curves were then employed, revealing a significant correlation between HCC survival and the metabolism of lactate along with the associated BCAAs. Additionally, a pivotal gene, NXPH4, implicated in lactate and BCAAs metabolism, was identified. The evidence presented strongly suggests that NXPH4 acts as a tumor promoter in the progression of HCC. Overall, our findings not only offer a reliable prognostic indicator for HCC but also shed light on the significance of lactate and BCAAs in the context of HCC. The identification of NXPH4 as a key player in these processes adds a layer of understanding to the molecular mechanisms involved in HCC progression, opening avenues for further research and potential therapeutic strategies.

Materials and methods

Cell culture

The LO2 cell line, representing normal human liver cells, and five other cell lines (HepG2, Huh7, Hep3B, MHCC97H, and SMMC-7721), along with human embryonic kidney (HEK) 29-3T cells, were obtained from the Cell Bank of the Chinese Academy of Sciences in Shanghai, China. These cells were carefully maintained in a controlled incubator at 37°C with a 5% CO2 atmosphere. The cell culture utilized DMEM (Dulbecco's Modified Eagle Medium) procured from Gibco in Grand Island, NY, USA. To ensure optimal growth conditions, 10% FBS (Fetal Bovine Serum) from the same source was added to the medium, providing essential nutrients and growth factors. Furthermore, a 1%

penicillin-streptomycin solution from Invitrogen in CA, USA, was introduced to the culture medium to prevent bacterial contamination and maintain a sterile environment.

Cell transfection

In the experimental framework, we strategically employed the Lipofectamine 3000 method, recognized for its proficiency in achieving efficient cell transfection, strictly following recommended guidelines from the manufacturer, Invitrogen (USA). The precise execution of this method by Genetong Biological organization (Xiamen, Fujian, China) involved integrating NXPH4 shRNA sequences into PLVX-shRNA vectors, designated as sh-NXPH4-1 and sh-NXPH4-2, with meticulous precision to meet the specific objectives of the experimental design. After successfully constructing these shRNA vectors, each containing the targeted NXPH4 shRNA sequences, they were co-transfected individually with pVSVG, pRRE, and pREV plasmids into HCC cells. Notably, the timing of this co-transfection process coincided with the cells reaching a critical confluence of 70%, optimized for the experiment. The cutting-edge Lipofectamine 3000 technology, along with its specialized chemicals, played a vital role in ensuring the efficiency and accuracy of the co-transfection process. To enrich the experimental scope further, we incorporated an overexpressing plasmid, pcDNA3.1-FOXK1, sourced from Genetong Biological Corporation (Xiamen, Fujian, China). This specific plasmid facilitated exploring FOXK1 overexpression dynamics within the experimental setup, providing valuable insights into the overall research objectives.

Quantitative real-time polymerase chain reaction (qRT-PCR)

The experimental process commenced with the isolation of total RNA using the well-established Trizol reagent from Thermo Fisher, adhering meticulously to the recommended protocols. Subsequently, the RNA underwent preparation through the Cytoplasmic & Nuclear RNA Purification kit, a product of Norgen Biotek based in Thorold, Canada. This step followed the precise guidelines provided by the manufacturer, ensuring the integrity and purity of the RNA samples. For the synthesis of complementary DNA (cDNA), 500 nanograms of the purified RNA were employed, utilizing the TaqMan cDNA synthesis kit from Thermo Fisher. The procedures outlined in the kit's protocols were diligently followed to guarantee the accuracy and efficiency of the cDNA synthesis process. In preparation for quantitative reverse transcription-polymerase chain reaction (qRT-PCR), the synthesized cDNA was combined with SYBR Green, a fluorophore from Solarbio located in Beijing, China. Primer pairs specific to the target genes were also included in the reaction mix. Applied Biosystems's ABI 7500 FAST Real-Time PCR System, located in Foster City, CA, USA, was used to perform the qRT-PCR studies. GAPDH was chosen as the endogenous reference gene for normalization, ensuring the accuracy of the relative quantification. The analysis of the relative RNA levels was carried out utilizing the 2-ΔΔCt method, providing a robust and standardized approach to assess gene expression changes within the experimental setup. RT-PCR for NXPH4 was carried out with the forward primer 5'-AAGGTCTTCGGACGGCCTA-3' and reverse primer 5'-GCAGCGAAAACTTGAGGGTAT-3'. GAPDH forward: 5'-TCCAGGAGCCGCACTTCTA-3' and reverse: 5'-CTCCGGGATGTGGATCTTCA-3'. FOXK1 forward: 5'-CCCGTGTCCCGTTGTTTTTC-3' and reverse: 5'-GCAACAGGTACGGACTTCCA-3'.

Cell viability assay

Cells (1×10^4 cells per well) were planted in 96-well plates (Nest Biotechnology) and nurtured with the designated concentration of substances for a duration of 12 hours. Following the treatment culmination, 10 μL of CCK-8 reagent was introduced into each well, succeeded by a 2-hour incubation at 37°C. The determination of cell viability ensued through the measurement of the absorbance value at 450 nm utilizing a microplate reader. Replication of each trial group occurred in triplicate. This study design encompasses cellular planting, exposure to defined chemical concentrations, a 2-hour incubation involving CCK-8 reagent, and the evaluation of cell viability through absorbance quantification at 450 nm using a microplate reader.

Colony formation

Transfected HepG2 and Huh7 cells were seeded at a density of 5×10^2 cells per well in 6-well plates and cultured for 2 weeks at 37°C. During

this incubation, the culture medium was refreshed every 4 days to maintain optimal cell conditions. Afterward, cells were thoroughly washed with PBS and fixed with 4% paraformaldehyde for 15 minutes at room temperature. Fixed cells were then stained with 0.5% crystal violet (Sigma-Aldrich, Merck KGaA) for 10 minutes at room temperature. Colony formation assessment, defined as clusters with more than 50 cells, was carried out using an optical microscope. This involved observing and counting distinct colonies formed by the transfected cells. This comprehensive experimental protocol facilitated a detailed analysis of the long-term growth and proliferation characteristics of transfected HepG2 and Huh7 cells.

Cell wound healing assay

A total of 100,000 cells per well were meticulously seeded into individual wells of a 6-well plate and nurtured in a complete medium. Upon reaching 75% confluence, a sterile pipette tip was employed to create consistent wounds across the cellular layers. Subsequently, the wounded cell layers underwent multiple phosphate-buffered saline (PBS) washes to eliminate any lingering cell debris. The cells were then subjected to additional incubation in a serum-free medium for a duration of 48 hours. During this incubation period, the cells demonstrated migration towards the wounded surface, depicting an in vitro healing phenomenon. The advancement of in vitro wound healing was captured using an inverted fluorescence microscope, and the closure rate was assessed. The healing rate was computed using the formula: [(initial wound width at 0 hours-wound width at 48 hours)/initial wound width at 0 hours] × 100%.

Transwell assay

Cells were exposed to varying concentrations of corylin a day before being placed into transwell chambers with an 8 μm pore size. Each well received 3 × 105 cells. The lower chamber was enriched with a 15% FBS concentration. After seeding and a 48-hour incubation, cells were precisely fixed with methanol for 30 minutes and subsequently stained using a 0.5% crystal violet solution for 20 minutes. Chambers underwent a comprehensive PBS washing, and cells in the upper chambers were gently detached. Microscopic analysis was utilized to capture cell visuals, and quantification was performed by tallying cell numbers.

Western blotting

Using the radioimmunoprecipitation assay lysis buffer supplied by Thermo Fisher, protein isolation was carried out from HepG2 and Huh7 cells. The bicinchoninic acid protein assay kit, manufactured by BioVision of San Francisco, CA, USA, was used to measure the amounts of the proteins that were extracted. The subsequent steps involved the separation of proteins on 10% sodium dodecyl sulfate-polyacrylamide gels, followed by their transfer onto polyvinylidene fluoride membranes (Thermo Fisher). After a brief incubation in 5% milk, the membranes were incubated overnight at 4°C with primary antibodies diluted 1:1000. The next step was to incubate the membranes for an additional hour at room temperature with 5% bovine serum albumin diluted to 1:5000 and horseradish peroxidase-conjugated anti-rabbit or anti-mouse secondary antibodies (BD Biosciences). Syngene systems and GeneSnap software, both developed by Syngene in Frederick, MD, USA, were subsequently used to assess the yielded protein bands.

In vivo assays

Athymic BALB/c nude mice (4-week old, male, weighing 16-18 g) were obtained from (Saiye Biology, Suzhou, China) and maintained in a specific pathogen-free (SPF) facility under controlled conditions (temperature: 22 ± 2°C, humidity: 50%-60%, 12-hour light/dark cycle) with free access to sterilized food and water. HepG2 cells in the logarithmic growth phase were harvested using trypsinization, washed twice with sterile PBS, and resuspended at a concentration of 1×10^7 cells/mL. For tumor formation assays, each mouse was subcutaneously injected with 0.2 mL of the cell suspension (containing 1×10^7 cells) into the right flank region using a 1 mL syringe with a 27-gauge needle. Mice were monitored daily for general health, behavior, and weight. Tumor volume was measured using digital calipers every seven days, and calculated using the formula: volume = (length × width^2)/2. After 4 weeks, mice were euthanized by cervical dislocation under anesthesia, and tumors were excised, photographed, and weighed. All experimental procedures were reviewed and approved by the

Committee on the Ethics of Animal Experiments of Henan Provincial People's Hospital and conducted in accordance with institutional guidelines and regulations for animal care and use.

ChIP assay

For ChIP tests, this research used Millipore Magna ChIP kits manufactured by YuSheng Biotech of Jinan, Shandong, China. After that, cells were harvested and DNA and protein crosslinks were created by applying formaldehyde for 15 minutes. After that, the cells were treated with a glycine buffer (10 × concentration) to remove the formaldehyde, which ended the crosslinking reaction. The next step was to use sonication to create DNA fragments with a range of 200 to 400 base pairs. The Abcam FOXK1 antibody, which was acquired from Qi-Bio in Wuhan, Hubei, China, was subsequently used to precipitate these DNA fragments. We used PTG anti-IgG antibodies from Wuhan, Hubei, China, as a hold-out. Lastly, the DNA fragments that precipitated were determined and quantified using qPCR analysis. This provided valuable information about the associations and interactions that were explored.

Luciferase reporter assays

The construction of various sequences related to the NXPH4 promoter was entrusted to Viraltherapy Technology in Wuhan, Hubei, China. Specifically, the wild-type (WT) of the NXPH4 promoter sequence, along with mutant sequences incorporating predicted binding site mutations, were separately integrated into pGL3 luciferase reporter plasmids. This process allowed for the creation of three distinct groups for luciferase reporter assays: the wild-type (WT) group and the MT group representing the mutant sequences. Following the plasmid constructions, co-transfections were performed using either pcDNA3.1 empty plasmids or pcDNA3.1-FOXK1 plasmids with the respective luciferase reporter plasmids from the wild-type (WT) and MT groups into 293T cells. After a 48-hour incubation period, cells from each group were harvested, and luciferase activities were determined using luciferase reporter kits from Promega in Pudong, Shanghai, China.

Glucose uptake and lactate secretion detection

The Glucose Uptake-Glo™ Assay kits from Promega in Pudong, Shanghai, China, were employed to assess glucose uptake in HCC cells under various treatment conditions. Briefly, HepG2 and Huh7 cells, post-treatment, were seeded in 96-well plates. After 24 hours, the cells were exposed to 2-deoxy-D-glucose (2DG) and incubated for 10 minutes. Subsequently, a sequential addition of stop buffer and neutralization buffer was performed. Following this, the 2DG6P Detection Reagent was introduced, and the cells were incubated for an additional 30 minutes. Luminescence detection was carried out using the GloMax® Navigator Microplate Luminometer from Promega in Pudong, Shanghai, China. Similarly, the Lactate-Glo™ Assay kits from Promega in Pudong, Shanghai, China, were utilized to detect lactate secretion based on the manufacturer's protocols. These assays provided valuable insights into the metabolic activities of HCC cells, particularly in terms of glucose uptake and lactate secretion, which are indicative of cellular metabolic alterations under different treatment conditions.

Acquisition of public data

The RNA-sequencing expression (level 3) and corresponding clinical information of liver hepatocellular carcinoma (LIHC) including 370 HCC samples and 50 paired normal samples were downloaded from database. The clinical characteristics of the HCC patients are temporarily provided in **Table 1**. In addition, the cell line mRNA expression matrix of tumors was obtained from the CCLE dataset. Meanwhile, 335 lactate metabolism-relate genes (LRGs) and 21 BCAA metabolism-related genes were acquired based on the GeneCards (https://www.genecards. org/) and Molecular Signatures Database (MSigDB, https://www.gsea-msigdb.org/gsea/msigdb/), respectively.

Consensus clustering

ConsensusClusterPlus, an R language package tailored for bioinformatics and data analysis, specializes in cluster analysis. Serving as an extension of ConsensusCluster, its primary goal is to identify highly consistent clustering structures, facilitating a better understanding of complex biological datasets. In this study, the expression patterns of lactate metabolism-related genes (LRGs) within HCC samples were examined using the "ConsensusClusterPlus" package. Additionally, subtypes related to BCAA metabolism were determined based on the ex-

Table 1. Association between high NXPH4 expression and several factors

Characteristics	Low expression of NXPH4	High expression of NXPH4	*P* value
n	185	185	
Gender, n (%)			0.0037
Female	45	72	
Male	140	113	
Age, n (%)			0.566
≤ 60	85	92	
> 60	100	94	
Pathologic stage, n (%)			0.00019
Stage I & Stage II	146	112	
Stage III & Stage IV	39	73	
Histologic grade, n (%)			
G1 & G2	126	109	0.066
G3 & G4	59	76	

pression profiles of BCAA metabolism-related genes. To validate these clustering results, Principal Component Analysis (PCA) was applied. Further analysis involved the use of the "Survival" package to compare overall survival (OS) among different subtypes. The investigation also included the creation of an expression heatmap depicting the gene expression patterns in various HCC subtypes. This comprehensive approach provided valuable insights into the distinct metabolic subtypes within HCC and their potential implications for patient survival.

Acquirement of differentially expressed genes (DEGs) in different subtypes

The limma package was employed to identify differentially expressed genes (DEGs) based on criteria of |log2FC| > 0.5 and p.adjusted < 0.05 within lactate metabolism-related subtypes and BCAA metabolism-related subtypes. The resulting DEGs were visualized using the "ggplot2" package to generate volcanic maps and heatmaps, with additional visualization carried out through the "pheatmap" package. Furthermore, Gene Ontology (GO) and Kyoto Encyclopedia of Genes and Genomes (KEGG) pathway enrichment analyses were conducted on the DEGs using the "clusterProfiler" R package. The outcomes of these analyses were presented using the "ggplot2" package. A detailed exploration of gene expression differences within lactate and BCAA metabolism-related subtypes was enabled by this comprehensive approach, illuminating their potential roles in biological processes.

Online bioinformatics analysis websites

The analysis in this study employed the Gene Set Cancer Analysis (GSCA) database (http://bioinfo.life.hust.edu.cn/GSCA/#/) to investigate gene expression, survivals (including OS, PFS, DSS), SNV, CNV, and methylation across various cancers based on The Cancer Genome Atlas (TCGA) data. The expression of NXPH4 in both pan-cancers was separately examined using the TIMER 2.0 database (http://timer.cistrome.org/). Additionally, KEGG pathway enrichment analysis was performed using the R software "ClusterProfiler", and the results were visualized by plotting the top 20 signaling pathways through the Chiplot website (https://www.chiplot.online/#).

Statistical analysis

The analysis was conducted using R software version 3.5.3. To assess the significance of differences between the risk score and clinicopathological characteristics, either a one-way ANOVA or Student's t-test was applied based on the specific context. Kaplan-Meier survival curves were skillfully crafted to explore potential disparities in survival between groups designated as high and low-risk. It is important to emphasize that all statistical assessments were two-sided, and a threshold of *P* value below 0.05 was considered to indicate statistical significance, unless explicitly stated otherwise.

Results

Identification of lactate metabolism subtypes and BCAA metabolic subtypes

The most effective clustering occurred when categorizing 370 HCC patients into two distinctive molecular subtypes (k = 2), as shown in **Figure 1A-C**. These groupings were established based on the expression patterns of genes related to lactate metabolism (LRGs). The visu-

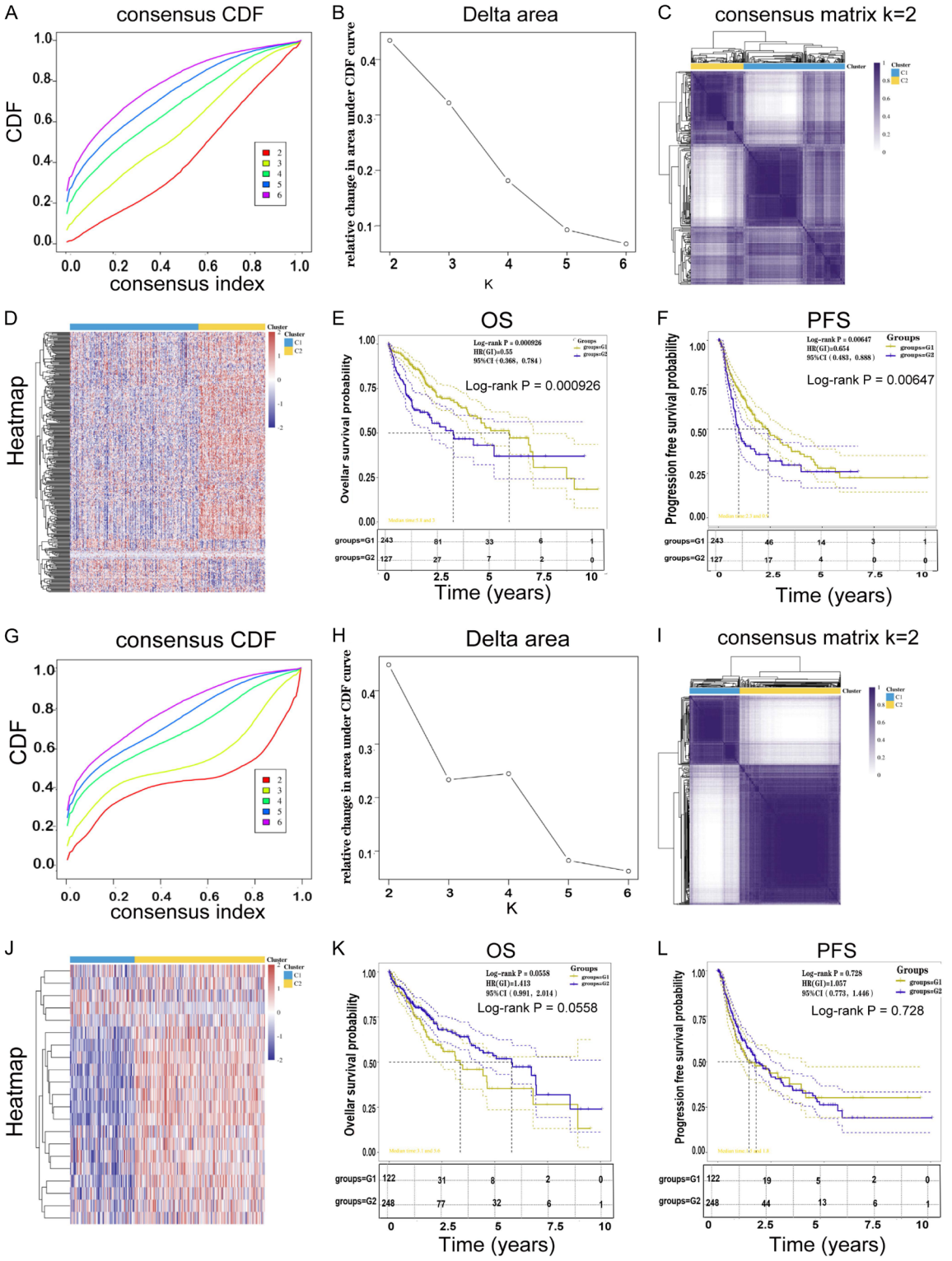

Figure 1. Identification of molecular subtypes based on lactate metabolism and Branched-Chain Amino Acid (BCAA) metabolism in Hepatocellular Carcinoma (HCC) Patients. A-C. Optimal clustering of 370 HCC patients into two distinct molecular subtypes (k = 2) based on the expression patterns of genes associated with lactate metabolism (LRGs). D. Visualization of lactate metabolism-related gene (LRG) expression differences among the identified molecular subtypes. The heatmap illustrates the relative expression levels of LRGs, highlighting the distinctive patterns within the identified subtypes. E, F. Prognostic implications of lactate metabolism-associated subtypes. G-L. Parallel examination of genes related to BCAA metabolism.

al representation of LRG expression differences among the identified subtypes is presented in **Figure 1D**. Remarkably, within the lactate metabolism-associated subtypes, cluster 2 demonstrated an unfavorable prognosis compared to cluster 1, depicted in **Figure 1E** and **1F**. Additionally, a parallel examination of genes related to BCAAS in **Figure 1G-L** supported similar observations.

Analysis of DEGs in different subtypes

In the lactate metabolism-associated subtypes, a total of 941 DEGs were uncovered, featuring 184 genes with increased expression and 757 with decreased expression, as illustrated in **Figure 2A** and **2B**. Meanwhile, among the subtypes related to BCAAs metabolism, a cohort of 518 DEGs surfaced, with 81 genes up-regulated and 437 genes down-regulated, depicted in **Figure 2C** and **2D**. Upon exploring the results of Gene Ontology (GO) and Kyoto Encyclopedia of Genes and Genomes (KEGG) analyses, it was apparent that the DEGs were primarily associated with pathways pertinent to tumors and metabolism, as visualized in **Figure 2E-H**.

Identification of prognostic LRG-BCAA-DGEs in HCC patients and pan-cancer analysis

A Venn diagram was employed to screen LRG-BCAA-DGEs specifically in HCC patients. The identification of 38 upregulated LRG-BCAA-DGEs in HCC patients is elucidated in **Figure 3A**. To delve deeper into their prognostic relevance, a Univariate analysis was conducted, unveiling 27 prognostic LRG-BCAA-DGEs in HCC patients. The Kaplan-Meier analysis underscored that all 27 prognostic LRG-BCAA-DGEs were inversely correlated with the long-term survival of HCC patients, as demonstrated in **Figure 3B** and **3C**. With the validation of 27 LRG-BCAA-DGEs in HCC, our investigation expanded to evaluate their expression and prognostic implications across diverse cancers. Differential expression analysis using the Gene Set Cancer Analysis (GSCA) database revealed that the majority of the 27 LRG-BCAA-DGEs exhibited heightened expression levels across pan-cancers, as depicted in **Figure 4A**. Furthermore, the exploration of the association between subtypes of various cancer types and the expressions of these 27 genes uncovered a subtype-specific expression pattern in breast cancer (BRCA), kidney renal clear cell carcinoma (KIRC), lung adenocarcinoma (LUAD), lung squamous cell carcinoma (LUSC), stomach adenocarcinoma (STAD), and others (**Figure 4B**). The trend of mRNA expression for these genes from early to late pathological stages was visualized by a trend plot, indicating up-regulation in late pathological stages across numerous tumor types (**Figure 4C**). Furthermore, the primary variation classification types of these genes predominantly comprised missense mutations, evident from the single nucleotide variant (SNV) summary graphic, with the most prevalent SNV class being C > T (**Figure 4D-F**). Copy number variation (CNV) analysis, a pivotal hallmark of cancer development, revealed that all 27 LRG-BCAA-DGEs exhibited numerous heterozygous copy number amplifications and deletions across the majority of cancer types. Additionally, homozygous CNV amplifications and deletions of these genes were observed in more than half of the cancer types, as demonstrated in **Figure 4G** and **4H**. In summary, the identified LRG-BCAA-DGEs show promise as potential biomarkers with prognostic value across various cancers, shedding light on their role in cancer development and progression. Further research and validation are warranted to elucidate the specific mechanisms underlying their influence on tumor biology and patient outcomes.

Methylation analysis of LRG-BCAA-DGEs in pan-cancers

Methylation is a biochemical process involving the addition of methyl groups to biomolecules. In living organisms, methylation typically refers to the methylation of DNA or proteins. Methylation is a complex and crucial biological modification that plays a vital role in regulating normal cellular functions and gene expression. Consequently, our attention turned to exploring the methylation patterns of the 27 LRG-BCAA-DGEs across a spectrum of cancers. **Figure 5A** illustrates the evaluation of methylation distinctions among the 27 LRG-BCAA-DGEs in various cancer types. Additionally, an examination of the correlation between methylation and mRNA expression of 23 LRG-BCAA-DGEs in pan-cancers revealed a prevailing negative correlation in most cancer types, as shown in **Figure 5B**. The investigation extended to HCC, where a consistent negative correlation was observed. Specifically, all 23 LRG-BCAA-DGEs mRNA ex-

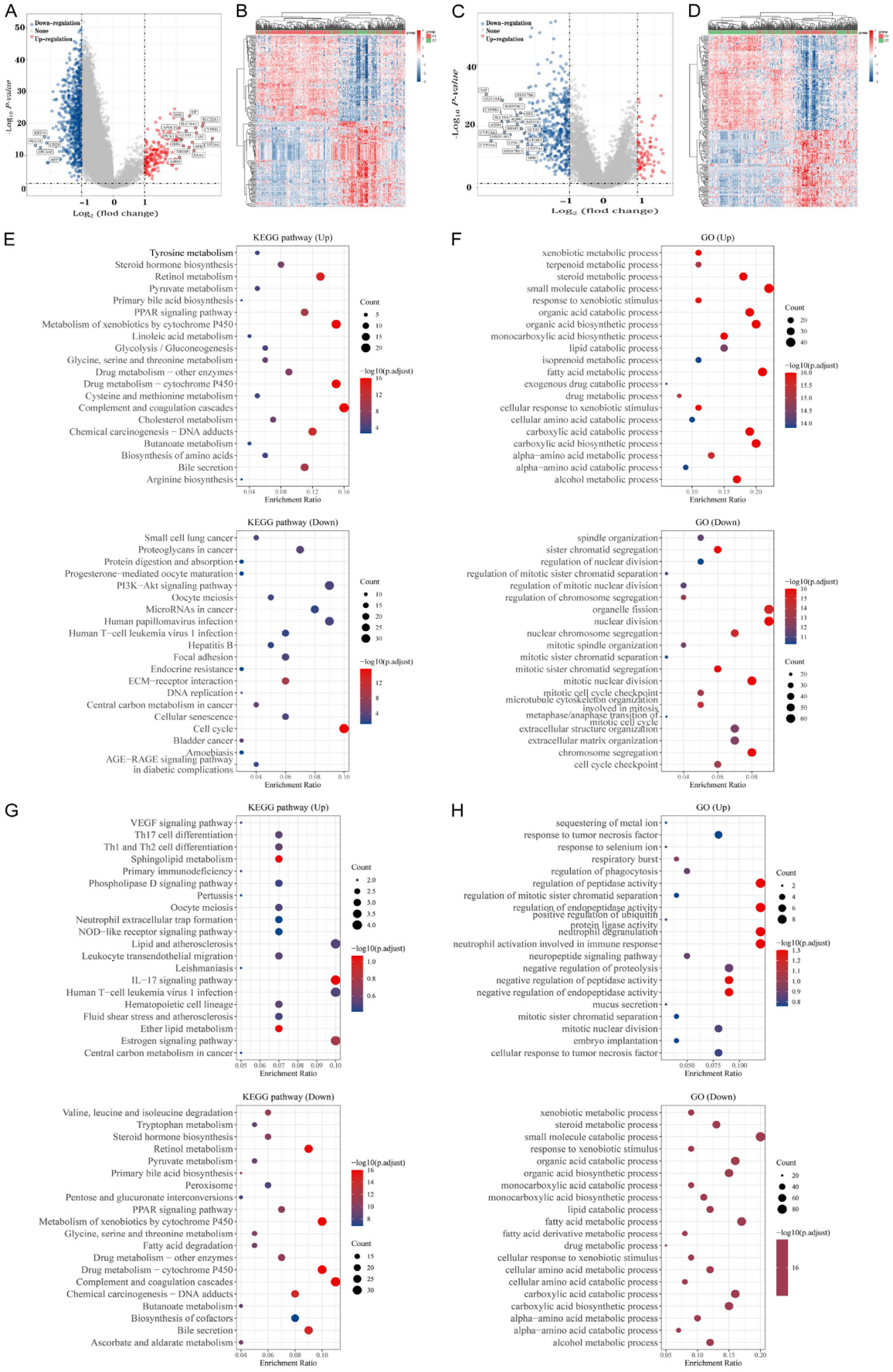
A
Down-regulation
None
Up-regulation
-Log10 P-value
Log2 (flod change)
B
C
Down-regulation
None
Up-regulation
-Log10 P-value
Log2 (flod change)
D
E
KEGG pathway (Up)
Tyrosine metabolism
Steroid hormone biosynthesis
Retinol metabolism
Pyruvate metabolism
Primary bile acid biosynthesis
PPAR signaling pathway
Metabolism of xenobiotics by cytochrome P450
Linoleic acid metabolism
Glycolysis / Gluconeogenesis
Glycine, serine and threonine metabolism
Drug metabolism – other enzymes
Drug metabolism – cytochrome P450
Cysteine and methionine metabolism
Complement and coagulation cascades
Cholesterol metabolism
Chemical carcinogenesis – DNA adducts
Butanoate metabolism
Biosynthesis of amino acids
Bile secretion
Arginine biosynthesis
Enrichment Ratio
Count
−log10(p.adjust)
KEGG pathway (Down)
Small cell lung cancer
Proteoglycans in cancer
Protein digestion and absorption
Progesterone−mediated oocyte maturation
PI3K−Akt signaling pathway
Oocyte meiosis
MicroRNAs in cancer
Human papillomavirus infection
Human T−cell leukemia virus 1 infection
Hepatitis B
Focal adhesion
Endocrine resistance
ECM−receptor interaction
DNA replication
Central carbon metabolism in cancer
Cellular senescence
Cell cycle
Bladder cancer
Amoebiasis
AGE−RAGE signaling pathway in diabetic complications
Enrichment Ratio
Count
−log10(p.adjust)
F
GO (Up)
xenobiotic metabolic process
terpenoid metabolic process
steroid metabolic process
small molecule catabolic process
response to xenobiotic stimulus
organic acid catabolic process
organic acid biosynthetic process
monocarboxylic acid biosynthetic process
lipid catabolic process
isoprenoid metabolic process
fatty acid metabolic process
exogenous drug catabolic process
drug metabolic process
cellular response to xenobiotic stimulus
cellular amino acid catabolic process
carboxylic acid catabolic process
carboxylic acid biosynthetic process
alpha−amino acid metabolic process
alpha−amino acid catabolic process
alcohol metabolic process
Enrichment Ratio
Count
−log10(p.adjust)
GO (Down)
spindle organization
sister chromatid segregation
regulation of nuclear division
regulation of mitotic sister chromatid separation
regulation of mitotic nuclear division
regulation of chromosome segregation
organelle fission
nuclear division
nuclear chromosome segregation
mitotic spindle organization
mitotic sister chromatid separation
mitotic sister chromatid segregation
mitotic nuclear division
mitotic cell cycle checkpoint
microtubule cytoskeleton organization involved in mitosis
metaphase/anaphase transition of mitotic cell cycle
extracellular structure organization
extracellular matrix organization
chromosome segregation
cell cycle checkpoint
Enrichment Ratio
−log10(p.adjust)
Count
G
KEGG pathway (Up)
VEGF signaling pathway
Th17 cell differentiation
Th1 and Th2 cell differentiation
Sphingolipid metabolism
Primary immunodeficiency
Phospholipase D signaling pathway
Pertussis
Oocyte meiosis
Neutrophil extracellular trap formation
NOD−like receptor signaling pathway
Lipid and atherosclerosis
Leukocyte transendothelial migration
Leishmaniasis
IL−17 signaling pathway
Human T−cell leukemia virus 1 infection
Hematopoietic cell lineage
Fluid shear stress and atherosclerosis
Ether lipid metabolism
Estrogen signaling pathway
Central carbon metabolism in cancer
Enrichment Ratio
Count
−log10(p.adjust)
KEGG pathway (Down)
Valine, leucine and isoleucine degradation
Tryptophan metabolism
Steroid hormone biosynthesis
Retinol metabolism
Pyruvate metabolism
Primary bile acid biosynthesis
Peroxisome
Pentose and glucuronate interconversions
PPAR signaling pathway
Metabolism of xenobiotics by cytochrome P450
Glycine, serine and threonine metabolism
Fatty acid degradation
Drug metabolism – other enzymes
Drug metabolism – cytochrome P450
Complement and coagulation cascades
Chemical carcinogenesis – DNA adducts
Butanoate metabolism
Biosynthesis of cofactors
Bile secretion
Ascorbate and aldarate metabolism
Enrichment Ratio
−log10(p.adjust)
Count
H
GO (Up)
sequestering of metal ion
response to tumor necrosis factor
response to selenium ion
respiratory burst
regulation of phagocytosis
regulation of peptidase activity
regulation of mitotic sister chromatid separation
regulation of endopeptidase activity
positive regulation of ubiquitin protein ligase activity
neutrophil degranulation
neutrophil activation involved in immune response
neuropeptide signaling pathway
negative regulation of proteolysis
negative regulation of peptidase activity
negative regulation of endopeptidase activity
mucus secretion
mitotic sister chromatid separation
mitotic nuclear division
embryo implantation
cellular response to tumor necrosis factor
Enrichment Ratio
Count
−log10(p.adjust)
GO (Down)
xenobiotic metabolic process
steroid metabolic process
small molecule catabolic process
response to xenobiotic stimulus
organic acid catabolic process
organic acid biosynthetic process
monocarboxylic acid catabolic process
monocarboxylic acid biosynthetic process
lipid catabolic process
fatty acid metabolic process
fatty acid derivative metabolic process
drug metabolic process
cellular response to xenobiotic stimulus
cellular amino acid metabolic process
cellular amino acid catabolic process
carboxylic acid catabolic process
carboxylic acid biosynthetic process
alpha−amino acid metabolic process
alpha−amino acid catabolic process
alcohol metabolic process
Enrichment Ratio
Count
−log10(p.adjust)

Figure 2. Analysis of Differentially Expressed Genes (DEGs) in lactate metabolism-associated and Branched-Chain Amino Acid (BCAA) Metabolism-Associated Subtypes of HCC Patients. A and B. Identification of DEGs in lactate metabolism-associated subtypes: a total of 941 degs were identified. C and D. Identification of DEGs in BCAA Metabolism-associated subtypes. E-H. Functional enrichment analysis of DEGs: results of GO and KEGG analyses illustrating the primary pathways associated with the identified DEGs.

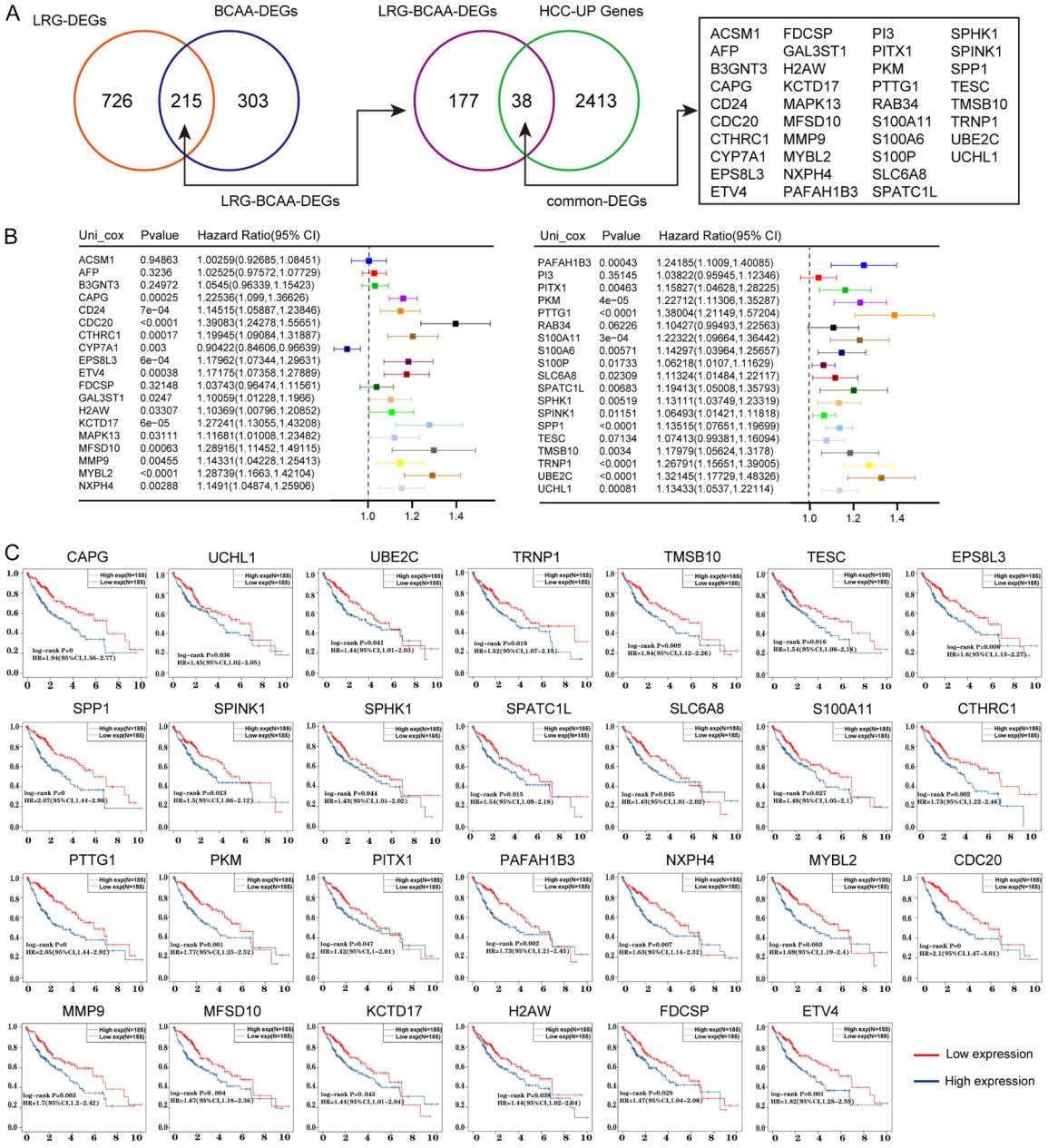

Figure 3. Identification and prognostic analysis of lactate metabolism and Branched-Chain Amino Acid (BCAA) metabolism-related genes in Hepatocellular Carcinoma (HCC) Patients. A. Venn diagram depicting the overlap of essential genes associated with lactate metabolism (LRGs) and branched-chain amino acid metabolism (DGEs) in HCC patients. B and C. Prognostic Analysis of LRG-BCAA-DGEs in HCC Patients by Univariate analysis and Kaplan-Meier analysis.

pression levels in liver LIHC exhibited a pronounced inverse correlation with their respective methylation levels (**Figure 5C**). Furthermore, an exploration of the impact of methylation dif-

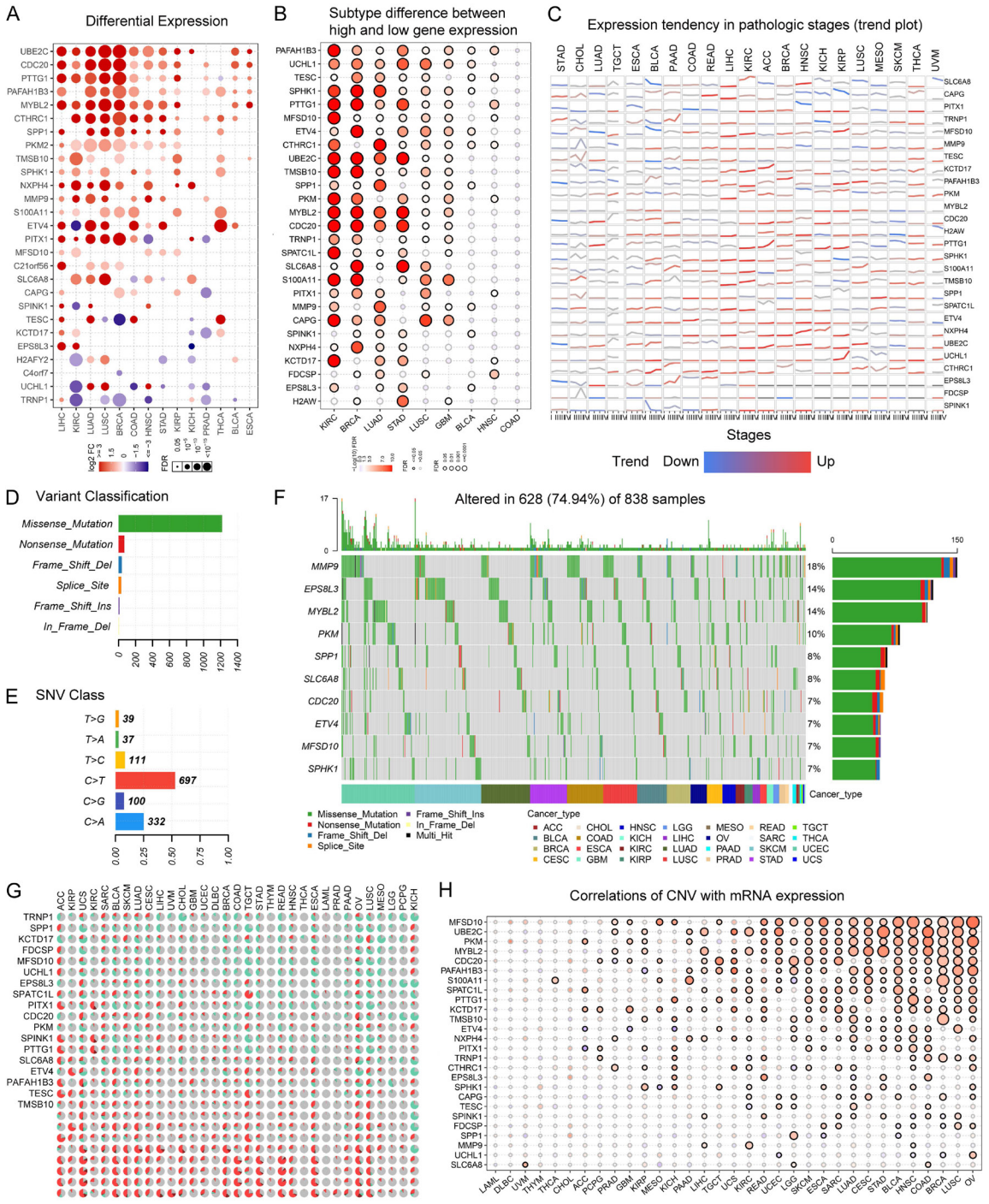

Figure 4. Expression and prognostic analysis of lactate metabolism and Branched-Chain Amino Acid (BCAA) metabolism-related genes across various cancers. A. Pan-cancer Differential Expression Analysis: using the Gene Set Cancer Analysis (GSCA) database. B. Subtype-Specific Expression Pattern. C. Visualization of the trend of mRNA expression for the identified genes across early to late pathological stages in various tumor types. D. Overall Survival Analysis. D-F. Single Nucleotide Variant (SNV) summary graphic: predominant variation classification types of these genes, with missense mutations highlighted, and the most prevalent SNV class being C > T. G, H. Copy Number Variation (CNV) Analysis.

ferences on survival outcomes (including overall survival (OS), progression-free survival (PFS), and disease-specific survival (DSS)) between high and low methylation states in each cancer

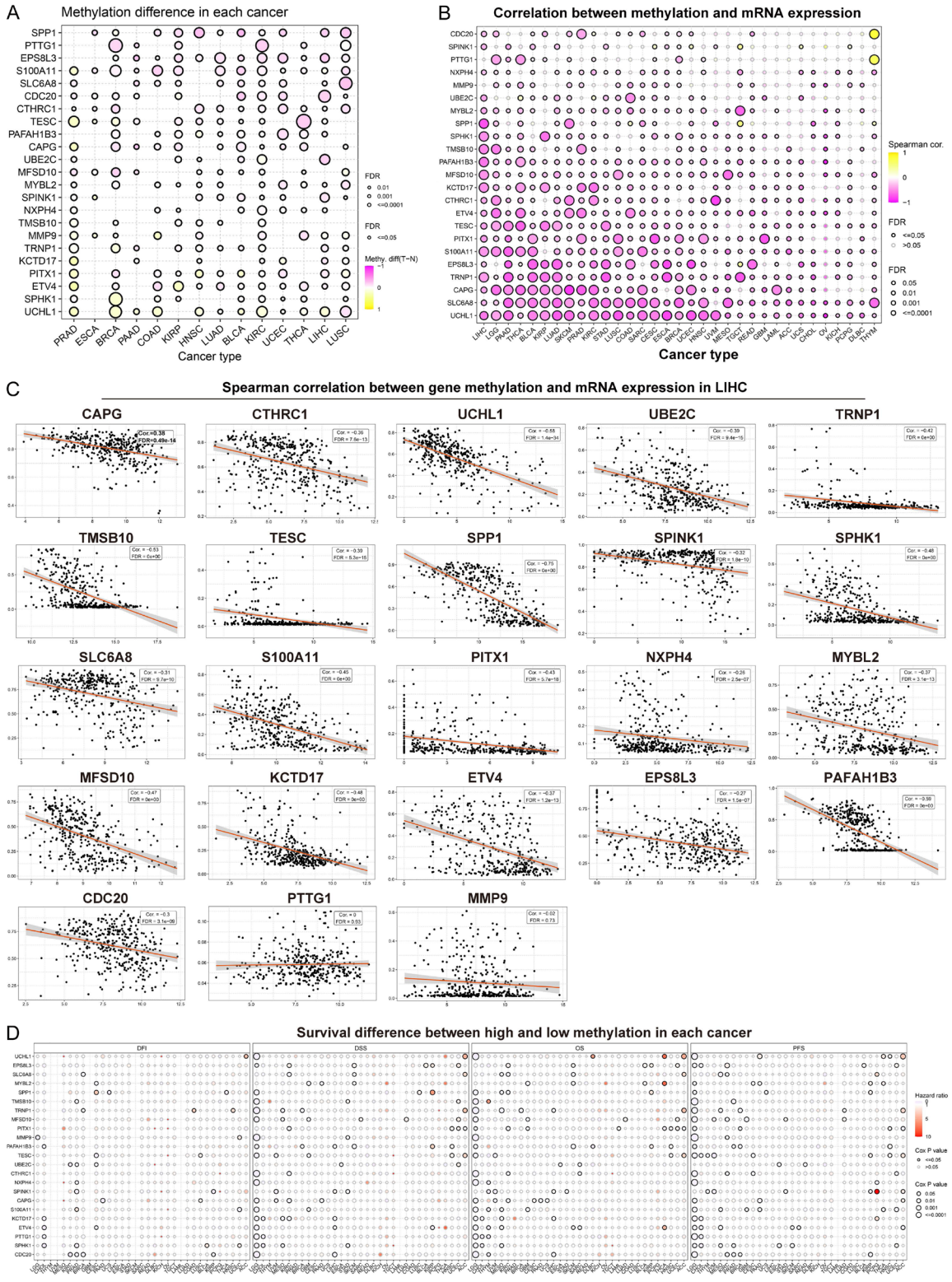

Figure 5. Methylation patterns and correlation analysis of LRG-BCAA-DGEs across Cancers. A. Evaluation of methylation distinctions among the 27 LRG-BCAA-DGEs in various cancer types. B. Examination of the correlation between methylation and mRNA expression of 23 LRG-BCAA-DGEs in pan-cancers. C. Investigation of the correlation between methylation and mRNA expression levels of 23 LRG-BCAA-DGEs in HCC. D. Impact on survival outcomes.

was conducted. The findings indicated that, for most cancer types, the methylation distinctions of the 23 LRG-BCAA-DGEs had limited effects on survival outcomes, with the exception of lower-grade glioma (LGG), as depicted in **Figure 5D**. In summary, the extensive analysis of methylation patterns across diverse cancers revealed a prevailing negative correlation between methylation and mRNA expression of the 23 LRG-BCAA-DGEs. Additionally, the influence of methylation differences on survival outcomes was relatively constrained across the majority of cancer types, underscoring the imperative for further investigation into the intricate relationship between methylation, gene expression, and cancer prognosis.

The expression and prognostic value of NXPH4 in HCC

Following the pan-cancer analysis, NXPH4 levels were found to be dysregulated across various tumor types, as shown in **Figure 6A**. This dysregulation was similarly observed in NXPH4 methylation patterns, as illustrated in **Figure 6B**. Further immune analysis unveiled associations between NXPH4 levels and numerous immune cell types in various tumors, as depicted in **Figure 6C-H**. In the subsequent focused examination of NXPH4 expression in HCC, heightened expression was confirmed in HCC specimens compared to non-tumor specimens, as presented in **Figure 7A**. Moreover, elevated NXPH4 expression positively correlated with advanced tumor grade and clinical stage, as showcased in **Figure 7B** and **7C**. The relationship between NXPH4 expression and molecular subtype, as well as immune subtype, is depicted in **Figure 7D** and **7E**. Additionally, the analysis revealed a negative association between NXPH4 levels and methylation, outlined in **Figure 7F** and **7G**. The 370 patients included in this study were categorized into high-risk and low-risk groups based on the median value of NXPH4 expression. Survival analysis outcomes indicated that patients with high NXPH4 expression exhibited shorter overall survival (OS) and progression-free survival (PFS) compared to those with low NXPH4 expression, as demonstrated in **Figure 7H** and **7I**. Further immune analysis revealed positive associations between NXPH4 levels and various immune cell types, including nTreg, NTK, B cells, and DC, as presented in **Figure 7J-M**. In conclusion, NXPH4 exhibits complex regulatory patterns, potentially playing a multifaceted role in cancer progression, prognosis, and interaction with the immune system. Further research is warranted to elucidate the specific mechanisms underlying NXPH4's involvement in different cancers and its potential as a therapeutic target or prognostic marker.

The biological functions of NXPH4 in HCC

After that, we isolated a variety of DEGs from individuals whose NXPH4 levels were either high or low. A total of 376 DEGs were screened (**Figure 8A** and **8B**). Moreover, the results of GSEA analysis revealed that 376 DEGs were mainly associated with endodermal cell differentiation, interleukin-10 production, positive regulation of small molecule metabolic process, cell cortex, cell projection membrane, centriolar satellite, acyl-CoA binding, acyltransferase activity and MHC class II protein complex binding (**Figure 8C-E**). Moreover, the results of KEGG analysis indicated that 376 DEGs were mainly associated with Drug metabolism - cytochrome P450, Metabolism of xenobiotics by cytochrome P450, Retinol metabolism and Chemical carcinogenesis - DNA adducts (**Figure 8F**). Importantly, the top 20 signaling pathway was shown in **Figure 8G**, including PPAR signaling pathway, PI3K-Akt signaling pathway, HIF-1 signaling pathway, Glucagon signaling pathway and Relaxin signaling pathway.

Knockdown of NXPH4 expression distinctly suppressed the proliferation, migration, invasion and EMT of HCC cells

We conducted both RT-PCR and Western blot analyses to evaluate NXPH4 expression levels in HCC cells. The results indicated a significant elevation of NXPH4 in five distinct HCC cell lines compared to LO2 cells, as depicted in **Figure 9A**. To delve deeper into the functional consequences of NXPH4, shRNA plasmids were utilized to efficiently suppress NXPH4 expression in HepG2 and Huh7 cells, achieving an efficacy of over 60%, as illustrated in **Figure 9B**. Functional assessments, encompassing CCK-8 and clonogenic assays, were then employed to scrutinize the effects of NXPH4 knockdown on the proliferation of HepG2 and Huh7 cells. The outcomes demonstrated a pronounced inhibition of cell proliferation in response to NXPH4 knockdown, as highlighted in **Figure 9C** and **9D**. Then, we next sought to investigate the roles of

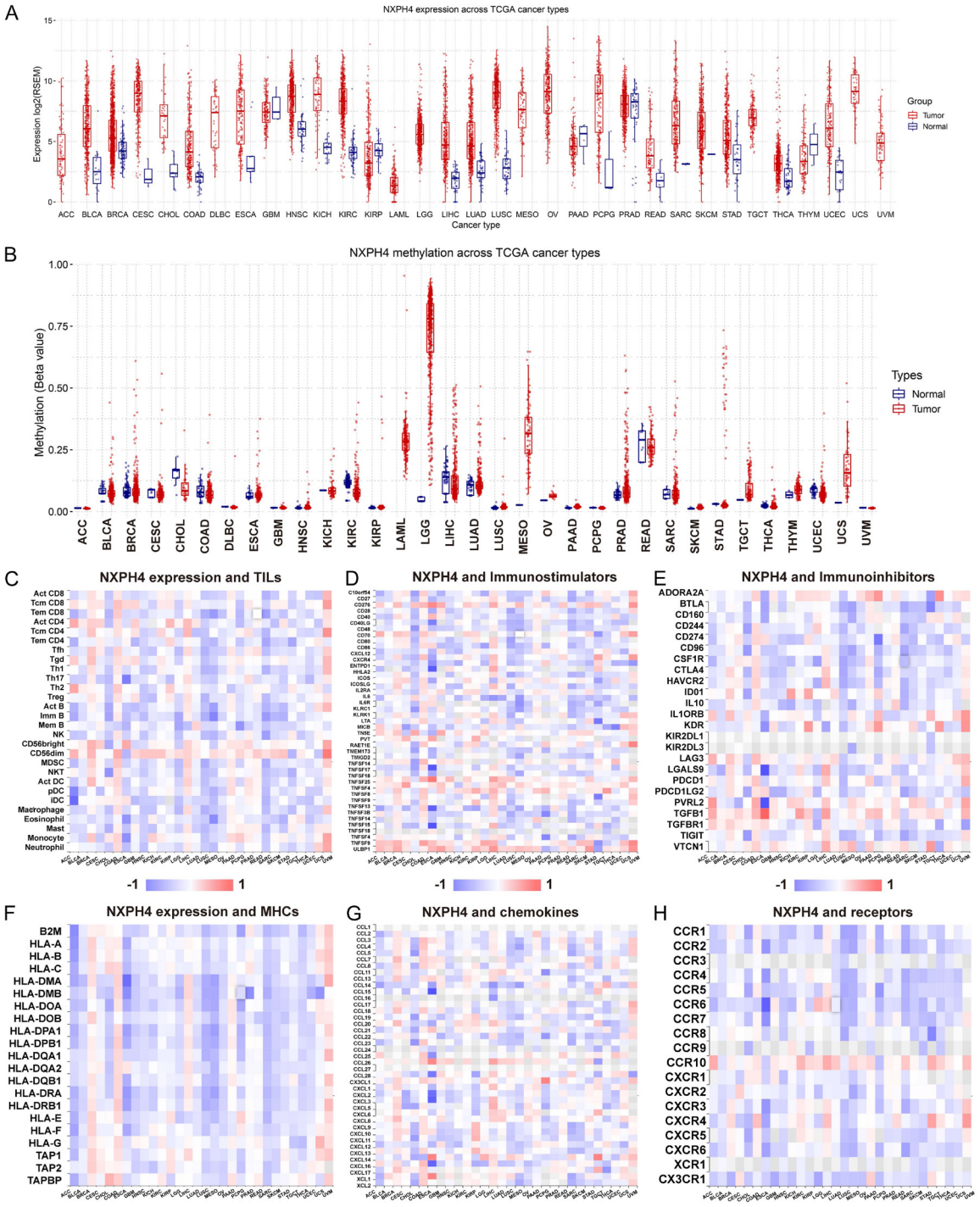

Figure 6. Expression, methylation, and immune analysis of NXPH4 across various tumor types. A. Dysregulation of NXPH4 Levels in pan-cancers. B. Illustration of NXPH4 methylation patterns, showcasing alterations in methylation levels across different tumor types. C-H. Comprehensive immune analysis revealing associations between NXPH4 levels and diverse immune cell types in various tumors.

NXPH4 in modulating HCC tumorigenesis in vivo. Firstly, we separately infected HepG2 cells with sh-NXPH4-1 and sh-NC lentivirus. Subsequently, the cells were collected and transplanted into nude mice. After four weeks, the tumor-bearing mice were sacrificed and the subcutaneous tumors were harvested. The tumors in the sh-NC group were remarkably larg-

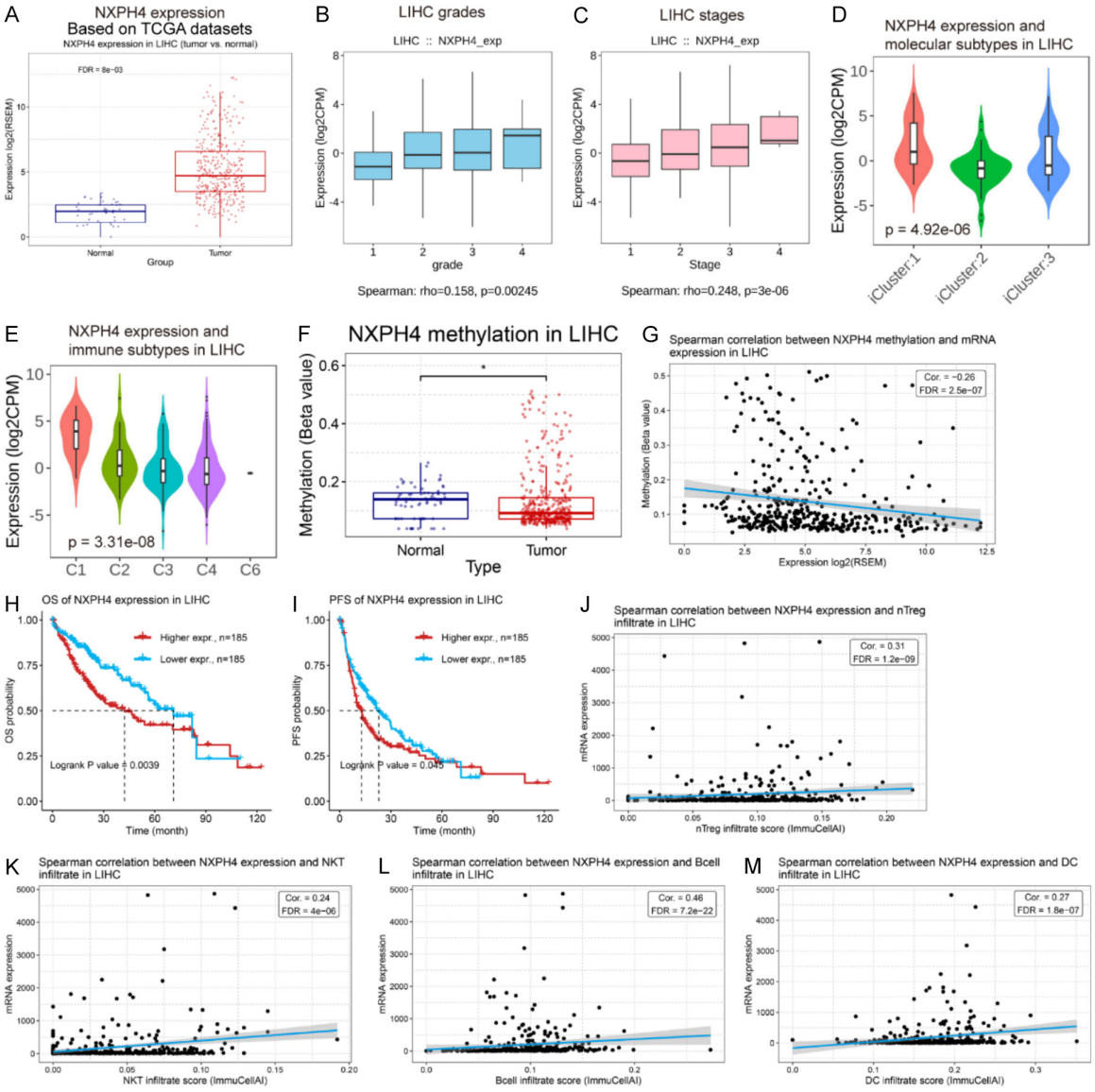

Figure 7. Comprehensive analysis of NXPH4 expression, clinical correlations, and immune associations in HCC. (A) Elevated Expression of NXPH4 in HCC. (B and C) Positive correlation between elevated NXPH4 expression and advanced tumor grade (B) and clinical stage (C) in HCC patients. (D and E) Illustration of the relationship between NXPH4 expression and molecular subtype (E) in HCC patients. (F and G) A negative association between NXPH4 levels and methylation patterns in HCC. (H and I) Outcome of survival analysis demonstrating that patients with high NXPH4 expression exhibit shorter overall survival (OS) and progression-free survival (PFS) compared to those with low NXPH4 expression in HCC. (J-M) Immune Cell Associations.

er than NXPH4 knockdown groups (**Figure 9E**). The results of tumor growth curves confirmed that NXPH4 depletion markedly reduced tumor volumes (**Figure 9F**). In addition, repressing NXPH4 expression resulted in significantly decreased tumor weights (**Figure 9G**). Additionally, we investigated the impact of NXPH4 on the migratory and invasive capabilities of HCC cells. Wound healing experiments showcased a substantial hindrance in cell migration upon NXPH4 knockdown, as displayed in **Figure 10A**. Transwell assays further corroborated these findings, revealing a diminished invasive ability of HepG2 and Huh7 cells following NXPH4 knockdown, as presented in **Figure 10B**. Moreover, we explored the expression levels of pivotal epithelial-mesenchymal transition (EMT) markers, including N-cadherin, E-cad-

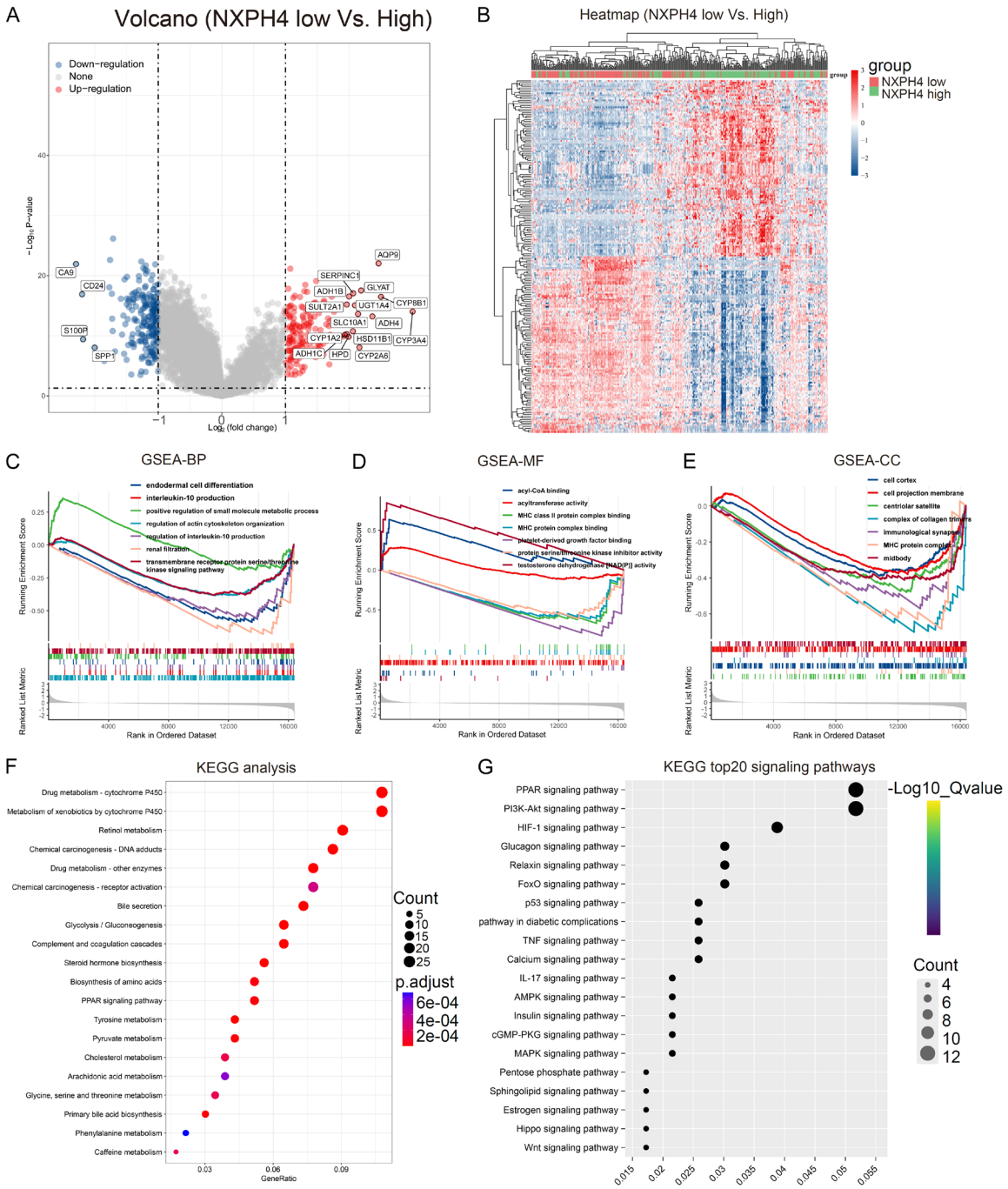

Figure 8. Functional analysis of DEGs Associated with NXPH4 Expression in HCC. (A and B) Isolation of 376 DEGs from HCC patients with varying levels of NXPH4 expression. (C-E) Gene Set Enrichment Analysis (GSEA): results of GSEA analysis depicting the enriched biological processes (C), cellular components (D), and molecular functions (E) associated with the 376 DEGs. (F) KEGG Pathway Analysis of 376 DEGs. (G) The top 20 signaling pathways.

herin, and Vimentin. The results indicated that the attenuation of NXPH4 led to a downregulation of N-cadherin and Vimentin expression, while concurrently upregulating E-cadherin expression, as demonstrated in **Figure 10C**. Collectively, these findings suggest that NXPH4 may exert a crucial role in modulating the proliferation, migration, and invasion of HCC cells, underscoring its potential as a therapeutic target in HCC treatment.

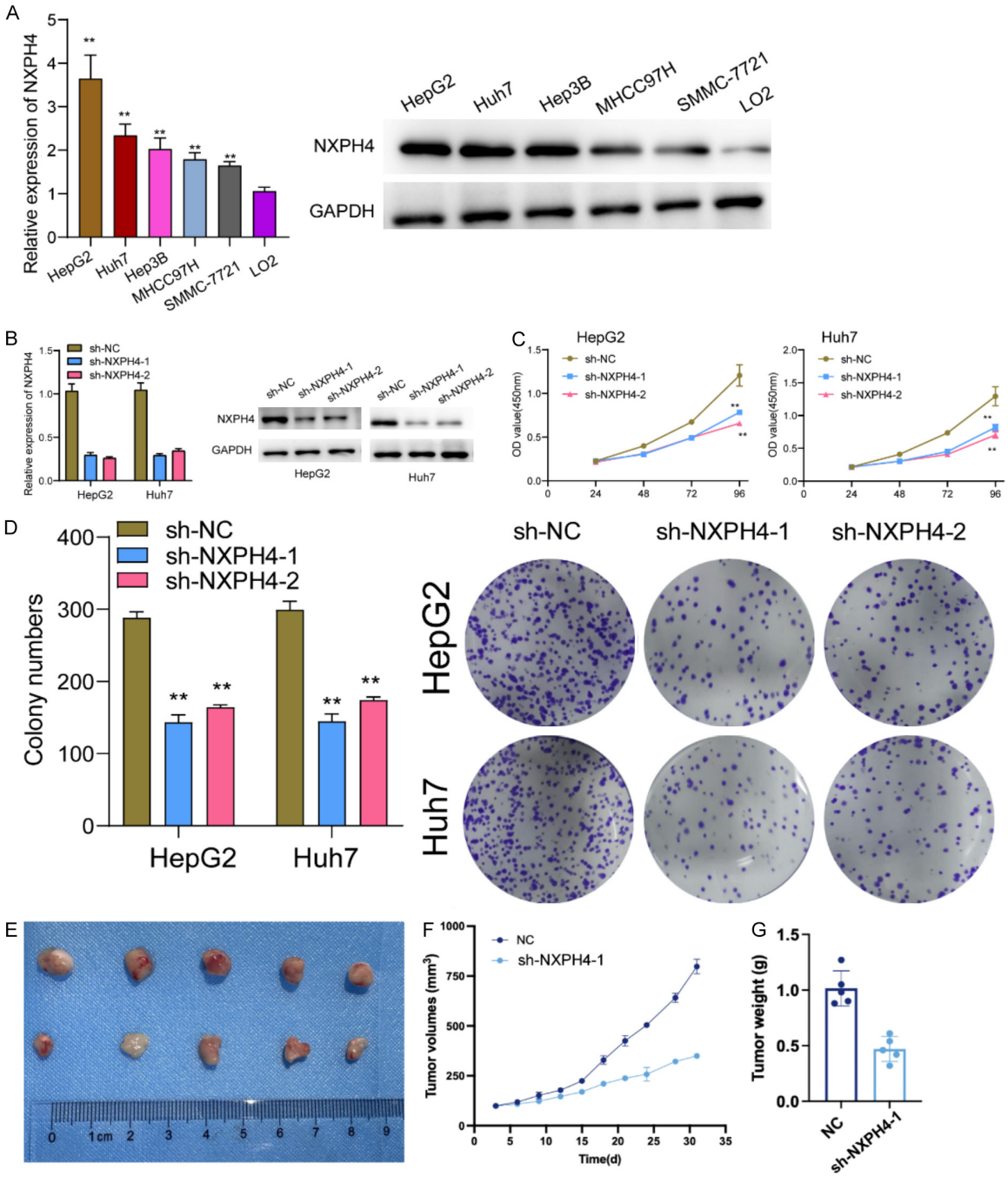

Figure 9. Knockdown of NXPH4 suppressed the proliferation of HCC cells. A. NXPH4 expression in HCC cell lines compared to LO2 cells using RT-PCR and Western blot analyses. B. Utilization of shRNA plasmids to efficiently suppress NXPH4 expression in HepG2 and Huh7 cells. C and D. Functional Assessments: CCK-8 and clonogenic assays employed to investigate the impact of NXPH4 knockdown on the proliferation of HepG2 and Huh7 cells. E. Images of whole tumors from the nude mice injected with HepG2 cells stably infected with sh-NC or sh-NXPH4-1. F. Effects of ZFPM2-AS1 depletion in HepG2 cells on subcutaneous tumor growth. Tumor volumes were measured every 4 days. G. Tumor weights were measured after the tumors were harvested from indicated groups. *P < 0.05, **P < 0.01.

NXPH4 modulates glucose uptake and lactate secretion via PI3K/Akt pathway in HCC cells

Given the significant correlation between NXPH4 dysregulation and cancer survival, particularly in HCC, our subsequent focus aimed to thoroughly investigate its role through experimental inquiries, aiming to uncover its functions in HCC tumorigenesis. Expanding our examination to the intricate link between NX-

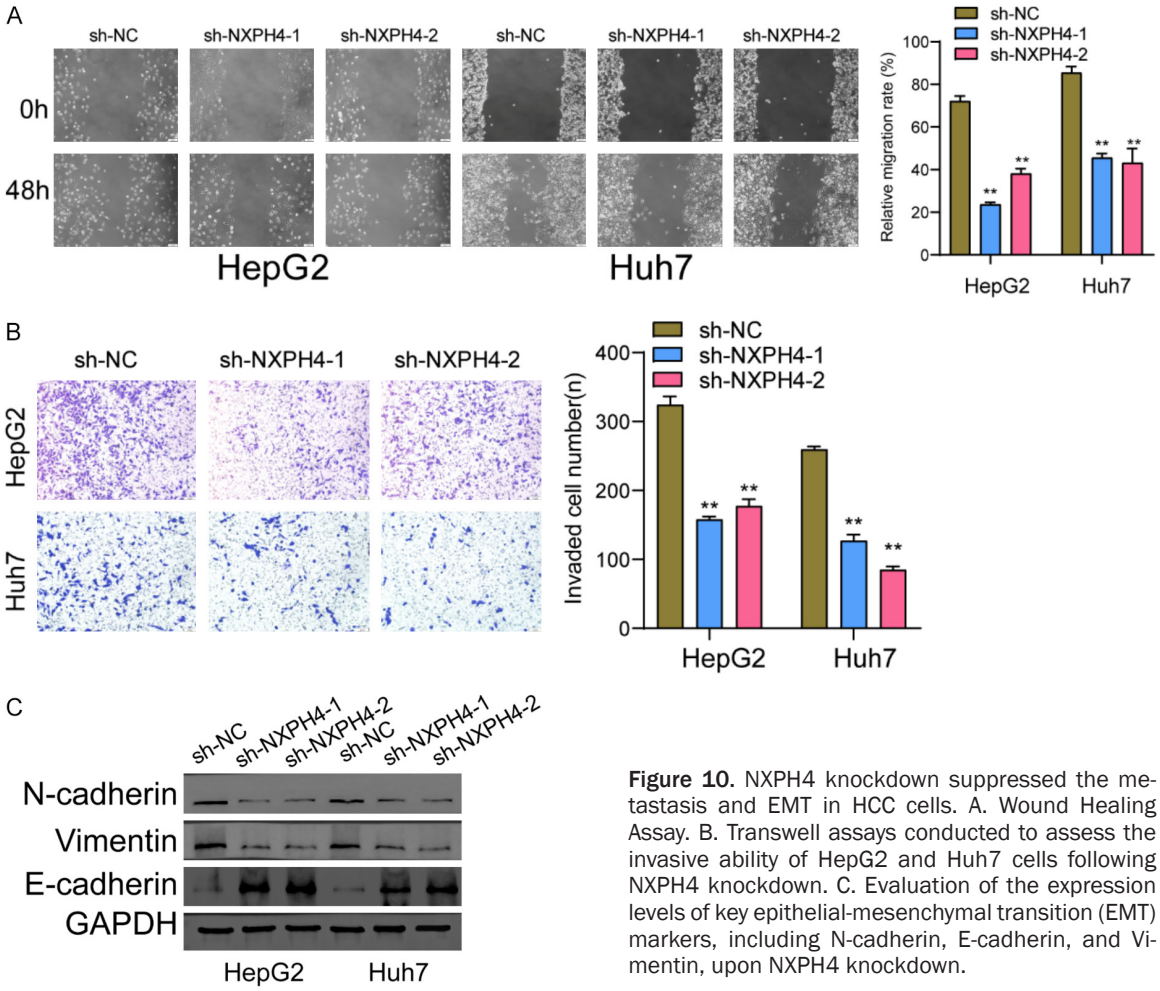

Figure 10. NXPH4 knockdown suppressed the metastasis and EMT in HCC cells. A. Wound Healing Assay. B. Transwell assays conducted to assess the invasive ability of HepG2 and Huh7 cells following NXPH4 knockdown. C. Evaluation of the expression levels of key epithelial-mesenchymal transition (EMT) markers, including N-cadherin, E-cadherin, and Vimentin, upon NXPH4 knockdown.

PH4 and glucose metabolism, we assessed glucose uptake and lactate secretion upon NXPH4 silencing. The results unequivocally revealed that decreased NXPH4 expression significantly curtailed both glucose uptake and lactate secretion, as depicted in **Figure 11A** and **11B**. Moreover, we conducted Western blot analyses to authenticate these findings, affirming that NXPH4 knockdown distinctly suppressed the expression of pivotal regulators of glucose metabolism, including GLUT1 and HK2, as illustrated in **Figure 11C**. In the concluding phase of our exploration, we delved into the potential molecular mechanisms underlying these observations, affirming that NXPH4 knockdown led to a suppression of PI3K and AKT phosphorylation, as evidenced by **Figure 11D**. These combined results offer valuable insights into the intricate molecular pathways through which NXPH4 exerts its influence on glucose metabolism in HCC, illuminating its potential as a therapeutic target in the context of HCC tumorigenesis.

FOXK1 directly targets NXPH4 promoter

To unravel the potential mechanisms driving the dysregulation of NXPH4 in HCC cells, we utilized the JASPAR database to predict binding sites for FOXK1 in the NXPH4 promoter region. The results uncovered a single potential binding site of FOXK1 in the NXPH4 promoter region, as depicted in **Figure 12A**. Subsequently, we evaluated the expression of FOXK1 in HepG2 and LO2 cells, confirming heightened expression in HepG2 cells, as demonstrated in **Figure 12B**. Additional validation through RT-PCR and Western blot confirmed that the transfection of Oe-FOXK1 distinctly upregulated FOXK1 expression in HepG2 cells, as illustrated in **Figure 12C**. To experimentally validate the binding capacity of FOXK1 to the predicted site, we gen-

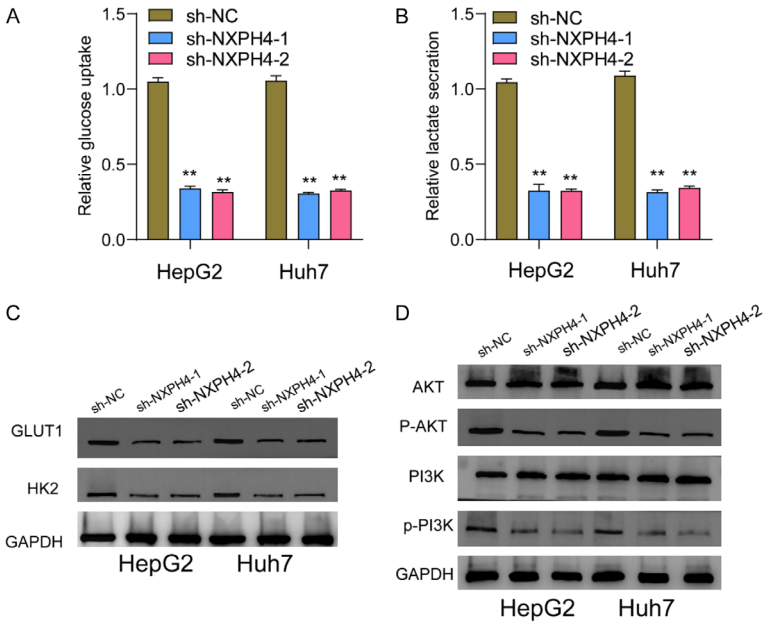

Figure 11. Functional insights into the role of NXPH4 in glucose metabolism in HCC. A. Assessment of glucose uptake in HCC cells upon NXPH4 silencing. B. Analysis of lactate secretion in HCC cells following NXPH4 knockdown. C. Western Blot Analysis for the expression of key regulators of glucose metabolism, including GLUT1 and HK2. D. Western blot for the expression of the related proteins of PI3K/Akt pathway in HCC cells.

erated wild-type (WT) and mutation (MT) luciferase reporter plasmids, as presented in **Figure 12D**. Luciferase reporter assays revealed that overexpressing FOXK1 increased the relative luciferase activity of the mutation binding site, indicating direct binding of FOXK1 to the NXPH4 promoter site, as shown in **Figure 12E**. Further confirmation was obtained through ChIP analysis, providing evidence that FOXK1 directly targets the NXPH4 promoter. Finally, we verified that the overexpression of FOXK1 distinctly downregulated the expression of NXPH4 in HepG2 cells, as depicted in **Figure 12F**. These findings collectively highlight FOXK1's direct targeting of the NXPH4 promoter, suggesting a potential regulatory mechanism contributing to NXPH4 dysregulation in HCC cells. These findings suggest that FOXK1 may act as a transcriptional regulator of NXPH4, providing insights into the molecular interactions that contribute to the dysregulation of NXPH4 in HCC. Further exploration of this FOXK1-NXPH4 regulatory axis may unravel additional complexities in HCC tumorigenesis, offering potential avenues for therapeutic intervention targeting this specific molecular pathway.

Discussion

Currently, clinical prognosis markers for HCC encompass a range of clinical, pathological, and molecular markers. Common markers include alpha-fetoprotein (AFP), carcinoembryonic antigen (CEA), and M2-pyruvate kinase (M2-PK) [25, 26]. However, these markers have limitations, such as low sensitivity, specificity issues, and susceptibility to false positives. Clinical staging based on TNM classification provides valuable information but lacks detailed molecular insights and may have reduced predictive capability for early-stage lesions [27, 28]. Molecular markers, including gene expression patterns and specific gene mutations (e.g., TP53, CTNNB1), offer more detailed information but face challenges related to heterogeneity and complex gene networks [29, 30]. The recent identification of lactate and BCAAs metabolism genes as potential indicators adds a promising avenue for prognosis assessment.

The relationship between lactate and BCAAs metabolism and cancer is intricately linked to altered cellular energetics, proliferation, and the modulation of the tumor microenvironment [31, 32]. Cancer cells exhibit aberrant metabolic features, where lactate and BCAAs play crucial roles in sustaining energy needs and supporting cell growth [18, 33]. The "Warburg effect" manifests as an increased production of lactate even in the presence of oxygen, providing cancer cells with essential energy for survival and proliferation through aerobic glycolysis. Simultaneously, alterations in BCAAs metabolism, including leucine, isoleucine, and valine, contribute to protein synthesis, signal transduction, and the regulation of cell proliferation [8, 34, 35]. These metabolic shifts not only fuel cancer cell survival and growth but also influence the tumor microenvironment. High levels of lactate contribute to tumor acidification, potentially promoting invasion and metastasis. Moreover, metabolites from BCAAs

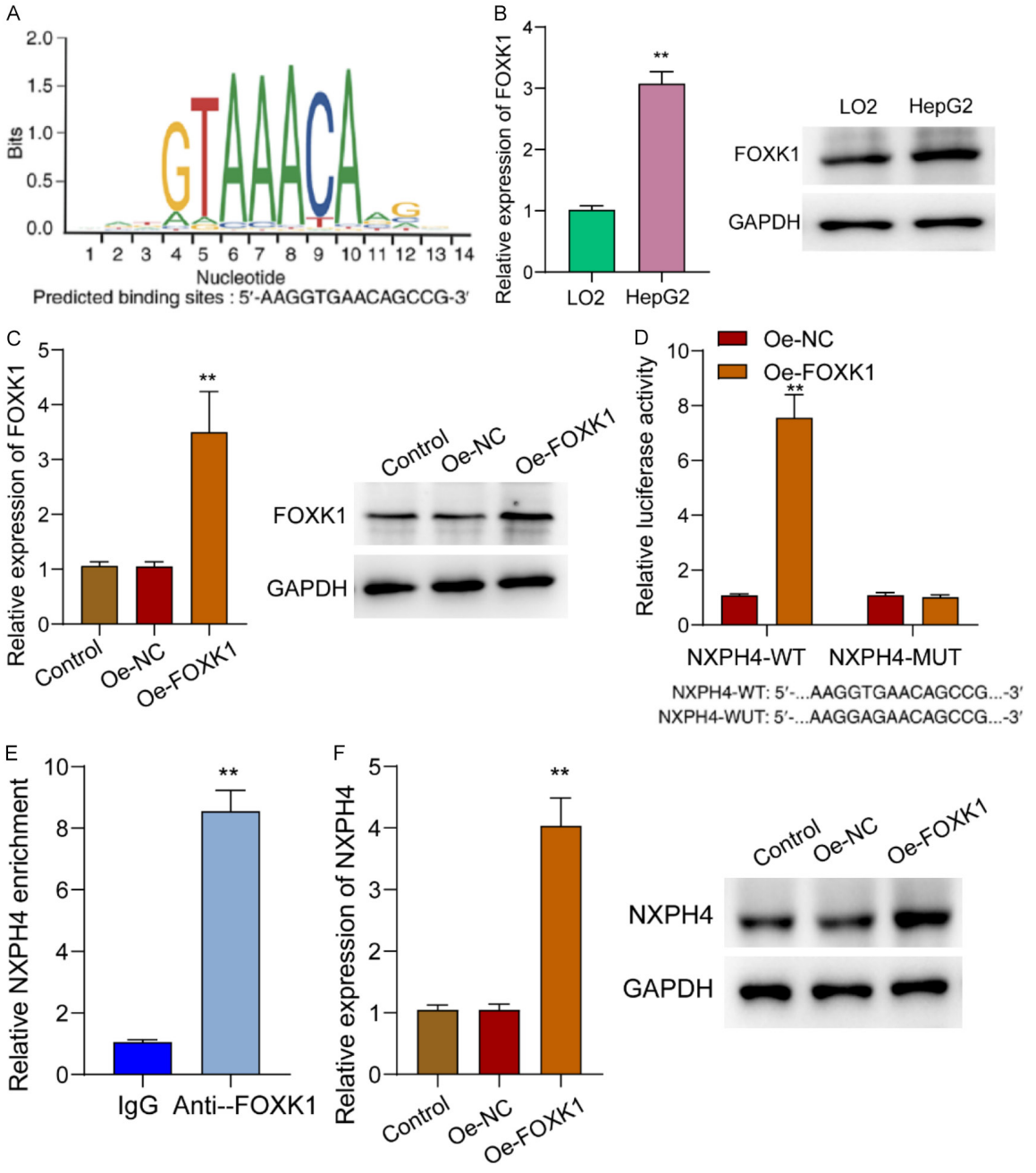

Figure 12. FOXK1 directly targets NXPH4 promoter in HCC cells. A. Utilizing the JASPAR database, a potential binding site of FOXK1 in the NXPH4 promoter region was predicted. B. FOXK1 Expression in HCC cells by western blot and RT-PCR. C. RT-PCR and Western blot validation of the transfection efficiency of Oe-FOXK1. D. Luciferase reporter assay: generation of wild-type (WT) and mutation (MT) luciferase reporter plasmids to experimentally validate FOXK1 binding. E. Confirmation of FOXK1's direct targeting of the NXPH4 promoter through ChIP analysis. F. Verification that overexpression of FOXK1 distinctly downregulated the expression of NXPH4 in HepG2 cells.

metabolism may play a role in tumor immune evasion. HCC employs multiple mechanisms to evade recognition and elimination by the immune system. These mechanisms include the upregulation of immune checkpoint molecules such as PD-L1 and CTLA-4, the recruitment of regulatory T cells (Tregs) and myeloid-derived suppressor cells (MDSCs), as well as the secretion of immunosuppressive cytokines such as TGF-β and IL-10. (Ning, J., Wang, Y. & Tao, Z. The complex role of immune cells in antigen presentation and regulation of T-cell respons-

es in hepatocellular carcinoma: progress, challenges, and future directions. Front. Immunol. 15, 1483834 (2024)). Research related to hepatocellular carcinoma (HCC) has demonstrated that CD4+ and CD8+ T cells within tumor tissues and ascitic fluid exhibit increased expression of TIM-3 and PD-1. Treatments targeting TIM-3 and PD-1 not only show significant antitumor efficacy individually, but their combined application enhances T cell infiltration into tumor tissues. (Zhang, X.-S. et al. Combined TIM-3 and PD-1 blockade restrains hepatocellular carcinoma development by facilitating CD4+ and CD8+ T cell-mediated antitumor immune responses. World J Gastrointest Oncol 15, 2138-2149 (2023)). The high level of the immunosuppressive molecule LAG-3 in HCC tumor tissues serves as a prognostic factor for survival. Notably, a high proportion of LAG-3+ and LAG-3+CD8+ cells prior to treatment is associated with improved survival outcomes in patients following immunotherapy. (Cheung, C. C. L. et al. Immunohistochemical scoring of LAG-3 in conjunction with CD8 in the tumor microenvironment predicts response to immunotherapy in hepatocellular carcinoma. Front. Immunol. 14, 1150985 (2023)). Recent research suggests that analyzing the expression of genes involved in these metabolic pathways can provide prognostic information for certain cancers [36, 37]. Understanding the intricate interplay between lactate and BCAAs metabolism and cancer holds promise for developing more effective therapeutic strategies by targeting these key metabolic pathways. Research has found that BCAA metabolism in adipocytes plays a significant role in glycolysis and lipogenesis during the differentiation of fat cells. Impairment of BCAA metabolism leads to a decrease in glycolytic; however, the cells can compensate by increasing the utilization of pyruvate. (Green, C. R. et al. Impaired branched-chain amino acid (BCAA) catabolism during adipocyte differentiation decreases glycolytic flux. Journal of Biological Chemistry 300, 108004 (2024)). This can explain the impact of BCAA metabolism on lactate metabolism. Research on HCC has revealed that elevated levels of BCAAs in the liver may have a carcinogenic effect. In comparison between liver cirrhosis and HCC, the levels of glutamate, α-tocopherol, valine, isoleucine, leucine, and cholesterol are found to be increased in HCC, whereas citrate, lactate, and sorbitol are downregulated in HCC. (Nezami Ranjbar, M. R. et al. GC-MS Based Plasma Metabolomics for Identification of Candidate Biomarkers for Hepatocellular Carcinoma in Egyptian Cohort. PLoS ONE 10, e0127299 (2015)). In this study, we identified distinct molecular subtypes based on lactate metabolism and BCAA pathways in 370 HCC patients. The clustering into two subtypes for both lactate metabolism and BCAA revealed notable differences in patient prognosis, with cluster 2 showing an unfavorable outcome. Further analysis identified a significant number of DEGs in each subtype, with enrichment in pathways related to tumors and metabolism. This suggests that the identified subtypes may have clinical relevance, offering insights into HCC progression and potential implications for personalized therapeutic approaches targeting specific metabolic pathways.

Moreover, we identified 27 prognostically significant genes among 38 upregulated LRG-BCAA-DGEs in HCC patients. Pan-cancer analysis revealed elevated expression of these genes across different cancers, displaying subtype-specific patterns. Notably, 12 LRG-BCAA-DGEs significantly influenced overall survival, particularly in kidney renal clear cell carcinoma (KIRC), liver hepatocellular carcinoma (LIHC), and lower-grade glioma (LGG). Methylation analysis indicated a negative correlation between methylation and mRNA expression across cancers, with limited effects on survival outcomes in most types, except for lower-grade glioma (LGG). These findings suggest the potential biological and clinical significance of these genes in HCC and other cancers, providing clues for a deeper understanding of their roles in tumor development and progression. Further research may help determine the application potential of these genes in personalized therapeutic strategies. Among the critical genes, our attention focused on NXPH4. We provided evidences that NXPH4 was highly expressed in HCC patients and associated with poor prognosis of HCC patients. More importantly, we performed functional assays and observed that NXPH4 was highly expressed in HCC cells and its knockdown distinctly suppressed the proliferation, metastasis and EMT pathway of HCC cells. These findings contribute to a deeper understanding of the specific pathways and processes influenced by NXPH4, providing a foundation for future research into the molecu-

lar intricacies of HCC. Ultimately, the characterization of NXPH4 as a key regulator in HCC opens up possibilities for tailored therapeutic interventions that could improve patient outcomes in the context of HCC.

Glucose uptake and lactate secretion play crucial roles in the development of liver cancer. Within cancer cells, there is a phenomenon known as the "Warburg effect", wherein cancer cells preferentially undergo glycolysis to produce lactate, even in the presence of oxygen, rather than utilizing the normal oxidative phosphorylation pathway [38, 39]. This results in an abnormal dependency of cancer cells on glucose, manifested by increased glucose uptake and corresponding lactate secretion. This phenomenon is also significantly evident in liver cancer. Cancer cells in the liver, aiming to meet their rapid proliferation and survival energy demands, enhance glucose uptake and sustain their metabolism by generating lactate through glycolysis [40, 41]. This abnormal metabolic pattern not only provides the necessary energy for cancer cells but may also impact the tumor microenvironment, leading to acidification and promoting invasion and metastasis of the tumor. Overall, glucose uptake and lactate secretion play pivotal roles in liver cancer development. Understanding the regulatory mechanisms of these metabolic processes contributes to a deeper comprehension of the biological characteristics of liver cancer, potentially providing targets for innovative therapeutic strategies aimed at disrupting these abnormal metabolic pathways to inhibit the growth and spread of liver cancer cells. In this study, we found that decreased NXPH4 expression significantly curtailed both glucose uptake and lactate secretion. It has been confirmed that the PI3K/Akt pathway exerts direct regulatory effects on glucose uptake. Activation of the PI3K/Akt pathway promotes the expression and transport of glucose transporter (GLUT), thereby enhancing cellular glucose uptake. Akt activation also leads to the phosphorylation of insulin receptor substrate 2 (IRS-2), facilitating the translocation of GLUT4 and increasing glucose internalization. Additionally, the PI3K/Akt pathway is involved in the regulation of lactate secretion. In malignant tumor cells, overactivation of the PI3K/Akt pathway promotes the progression of glycolysis, leading to increased production of lactate from glucose via glycolysis. Akt activation further influences the expression of key enzymes such as lactate dehydrogenase (LDH), contributing to an additional elevation in lactate production. In this study, we also confirmed that NXPH4 may modulate glucose uptake and lactate secretion via PI3K/Akt pathway in HCC cells.

Transcription factors are a class of proteins that play a crucial regulatory role within cells, particularly in the process of gene transcription [42, 43]. These proteins exert their influence by binding to specific regions of DNA, thereby impacting the transcriptional activity of nearby genes. Transcription factors can either promote or inhibit the transcription of genes to which they bind [44, 45]. They achieve this by regulating the activity of RNA polymerase or by interacting with other regulatory proteins. The activity of transcription factors is often subject to regulation by cellular signaling pathways. For instance, signaling molecules within the cell can activate or inhibit transcription factors, thereby modulating the expression of associated genes [46, 47]. In order to explore the potential mechanisms involved in NXPH4 dysregulation in HCC cells, we searched the JASPAR database and revealed a specific binding site for FOXK1 in the NXPH4 promoter. FOXK1 is a member of the FOX (Forkhead box) family of transcription factors. Transcription factors are proteins that play a crucial role in regulating gene expression, influencing various cellular processes. Previously, several studies have reported that FOXK1 was highly expressed in HCC cells and its knockdown suppressed the proliferation and metastasis of HCC cells. In this study, our results demonstrate direct binding of FOXK1 to the predicted NXPH4 promoter site. Overexpression of FOXK1 results in a significant downregulation of NXPH4 in HepG2 cells. These findings suggest FOXK1 acts as a transcriptional regulator of NXPH4, offering insights into the dysregulation of NXPH4 in HCC. The FOXK1-NXPH4 axis may represent a potential therapeutic target for HCC intervention.

This article has some limitations. Firstly, HCC patients in the article is primarily based on a sample of 370 individuals. This sample size is relatively small and may not comprehensively represent the diversity of all HCC patients. Larger-scale studies was needed to conduct a more comprehensive analysis across different populations and cases. Secondly, the article

relies solely on in vitro laboratory validation for exploring the functions of NXPH4. It is essential to further confirm its biological effects through additional cell lines and animal models. Thirdly, we identified potential biomarkers correlated with the prognosis of HCC patients. However, the clinical relevance of these results requires further validation through additional independent clinical studies to ensure the robustness and accuracy of these biomarkers in actual patients.

Conclusion

In conclusion, our study identified distinct lactate metabolism and BCAAs subtypes in 370 HCC patients, revealing significant prognostic differences between clusters. The analysis of DEGs associated with these subtypes highlighted their involvement in crucial tumor-related pathways. The prognostic significance of lactate metabolism and branched-chain amino acid-related genes was validated across diverse cancers, emphasizing their potential as biomarkers. NXPH4 emerged as a key player in HCC, demonstrating dysregulation across tumors, association with advanced stages, and a complex role in cancer progression and immune modulation. Moreover, our findings unveiled a novel regulatory axis involving FOXK1 targeting the NXPH4 promoter, shedding light on potential therapeutic avenues for HCC treatment.

Disclosure of conflict of interest

None.

Address correspondence to: Deyu Li, Department of Hepato-Biliary Pancreatic Surgery, Henan Provincial People's Hospital, No. 7 Weiwu Road, Zhengzhou, Henan, China. E-mail: lideyu0408@163.com

References

[1] Siegel RL, Miller KD, Wagle NS and Jemal A. Cancer statistics, 2023. CA Cancer J Clin 2023; 73: 17-48.

[2] Feng R, Su Q, Huang X, Basnet T, Xu X and Ye W. Cancer situation in China: what does the China cancer map indicate from the first national death survey to the latest cancer registration? Cancer Commun (Lond) 2023; 43: 75-86.

[3] Anwanwan D, Singh SK, Singh S, Saikam V and Singh R. Challenges in liver cancer and possible treatment approaches. Biochim Biophys Acta Rev Cancer 2020; 1873: 188314.

[4] Marengo A, Rosso C and Bugianesi E. Liver cancer: connections with obesity, fatty liver, and cirrhosis. Annu Rev Med 2016; 67: 103-117.

[5] Liu CY, Chen KF and Chen PJ. Treatment of liver cancer. Cold Spring Harb Perspect Med 2015; 5: a021535.

[6] Sia D, Villanueva A, Friedman SL and Llovet JM. Liver cancer cell of origin, molecular class, and effects on patient prognosis. Gastroenterology 2017; 152: 745-761.

[7] Sun JH, Luo Q, Liu LL and Song GB. Liver cancer stem cell markers: progression and therapeutic implications. World J Gastroenterol 2016; 22: 3547-3557.

[8] Li X, Yang Y, Zhang B, Lin X, Fu X, An Y, Zou Y, Wang JX, Wang Z and Yu T. Lactate metabolism in human health and disease. Signal Transduct Target Ther 2022; 7: 305.

[9] Rabinowitz JD and Enerbäck S. Lactate: the ugly duckling of energy metabolism. Nat Metab 2020; 2: 566-571.

[10] Brooks GA. The science and translation of lactate shuttle theory. Cell Metab 2018; 27: 757-785.

[11] van Gemert LA, de Galan BE, Wevers RA, Ter Heine R and Willemsen MA. Lactate infusion as therapeutical intervention: a scoping review. Eur J Pediatr 2022; 181: 2227-2235.

[12] Chen L, Huang L, Gu Y, Cang W, Sun P and Xiang Y. Lactate-lactylation hands between metabolic reprogramming and immunosuppression. Int J Mol Sci 2022; 23: 11943.

[13] Vincent JL, Quintairos E Silva A, Couto L Jr, and Taccone FS. The value of blood lactate kinetics in critically ill patients: a systematic review. Crit Care 2016; 20: 257.

[14] Brooks GA. Lactate as a fulcrum of metabolism. Redox Biol 2020; 35: 101454.

[15] Zhang Y, Zhai Z, Duan J, Wang X, Zhong J, Wu L, Li A, Cao M, Wu Y, Shi H, Zhong J and Guo Z. Lactate: the mediator of metabolism and immunosuppression. Front Endocrinol (Lausanne) 2022; 13: 901495.

[16] Wang ZH, Peng WB, Zhang P, Yang XP and Zhou Q. Lactate in the tumour microenvironment: from immune modulation to therapy. EBioMedicine 2021; 73: 103627.

[17] Brooks GA, Osmond AD, Arevalo JA, Duong JJ, Curl CC, Moreno-Santillan DD and Leija RG. Lactate as a myokine and exerkine: drivers and signals of physiology and metabolism. J Appl Physiol (1985) 2023; 134: 529-548.

[18] Neinast M, Murashige D and Arany Z. Branched chain amino acids. Annu Rev Physiol 2019; 81: 139-164.

[19] Plotkin DL, Delcastillo K, Van Every DW, Tipton KD, Aragon AA and Schoenfeld BJ. Isolated leucine and branched-chain amino acid supple-

mentation for enhancing muscular strength and hypertrophy: a narrative review. Int J Sport Nutr Exerc Metab 2021; 31: 292-301.
[20] Lynch CJ and Adams SH. Branched-chain amino acids in metabolic signalling and insulin resistance. Nat Rev Endocrinol 2014; 10: 723-736.
[21] Holeček M. Branched-chain amino acids in health and disease: metabolism, alterations in blood plasma, and as supplements. Nutr Metab (Lond) 2018; 15: 33.
[22] Wolfe RR. Branched-chain amino acids and muscle protein synthesis in humans: myth or reality? J Int Soc Sports Nutr 2017; 14: 30.
[23] Kim WK, Singh AK, Wang J and Applegate T. Functional role of branched chain amino acids in poultry: a review. Poult Sci 2022; 101: 101715.
[24] Sivanand S and Vander Heiden MG. Emerging roles for branched-chain amino acid metabolism in cancer. Cancer Cell 2020; 37: 147-156.
[25] Cao W, Xing H, Li Y, Tian W, Song Y, Jiang Z and Yu J. Claudin18.2 is a novel molecular biomarker for tumor-targeted immunotherapy. Biomark Res 2022; 10: 38.
[26] Vogel A, Meyer T, Sapisochin G, Salem R and Saborowski A. Hepatocellular carcinoma. Lancet 2022; 400: 1345-1362.
[27] Sangro B, Sarobe P, Hervás-Stubbs S and Melero I. Advances in immunotherapy for hepatocellular carcinoma. Nat Rev Gastroenterol Hepatol 2021; 18: 525-543.
[28] Singal AG, Lampertico P and Nahon P. Epidemiology and surveillance for hepatocellular carcinoma: new trends. J Hepatol 2020; 72: 250-261.
[29] Wang Y and Deng B. Hepatocellular carcinoma: molecular mechanism, targeted therapy, and biomarkers. Cancer Metastasis Rev 2023; 42: 629-652.
[30] Greten TF, Villanueva A, Korangy F, Ruf B, Yarchoan M, Ma L, Ruppin E and Wang XW. Biomarkers for immunotherapy of hepatocellular carcinoma. Nat Rev Clin Oncol 2023; 20: 780-798.
[31] Mero A. Leucine supplementation and intensive training. Sports Med 1999; 27: 347-358.
[32] Martinho DV, Nobari H, Faria A, Field A, Duarte D and Sarmento H. Oral branched-chain amino acids supplementation in athletes: a systematic review. Nutrients 2022; 14: 4002.
[33] Nie C, He T, Zhang W, Zhang G and Ma X. Branched chain amino acids: beyond nutrition metabolism. Int J Mol Sci 2018; 19: 954.
[34] He J, Shi H, Li X, Nie X, Yang Y, Li J, Wang J, Yao M, Tian B and Zhou J. A review on microbial synthesis of lactate-containing polyesters. World J Microbiol Biotechnol 2022; 38: 198.
[35] Luo Y, Li L, Chen X, Gou H, Yan K and Xu Y. Effects of lactate in immunosuppression and inflammation: progress and prospects. Int Rev Immunol 2022; 41: 19-29.
[36] Doherty JR and Cleveland JL. Targeting lactate metabolism for cancer therapeutics. J Clin Invest 2013; 123: 3685-3692.
[37] Adeva-Andany M, López-Ojén M, Funcasta-Calderón R, Ameneiros-Rodríguez E, Donapetry-García C, Vila-Altesor M and Rodríguez-Seijas J. Comprehensive review on lactate metabolism in human health. Mitochondrion 2014; 17: 76-100.
[38] Ye L, Jiang Y and Zhang M. Crosstalk between glucose metabolism, lactate production and immune response modulation. Cytokine Growth Factor Rev 2022; 68: 81-92.
[39] Martinez-Outschoorn UE, Peiris-Pagés M, Pestell RG, Sotgia F and Lisanti MP. Cancer metabolism: a therapeutic perspective. Nat Rev Clin Oncol 2017; 14: 11-31.
[40] Legouis D, Faivre A, Cippà PE and de Seigneux S. Renal gluconeogenesis: an underestimated role of the kidney in systemic glucose metabolism. Nephrol Dial Transplant 2022; 37: 1417-1425.
[41] Bose S and Le A. Glucose metabolism in cancer. Adv Exp Med Biol 2018; 1063: 3-12.
[42] Lambert SA, Jolma A, Campitelli LF, Das PK, Yin Y, Albu M, Chen X, Taipale J, Hughes TR and Weirauch MT. The human transcription factors. Cell 2018; 172: 650-665.
[43] Deng C, Wu Y, Lv X, Li J, Liu Y, Du G, Chen J and Liu L. Refactoring transcription factors for metabolic engineering. Biotechnol Adv 2022; 57: 107935.
[44] Jiang J, Ma S, Ye N, Jiang M, Cao J and Zhang J. WRKY transcription factors in plant responses to stresses. J Integr Plant Biol 2017; 59: 86-101.
[45] Vaquerizas JM, Kummerfeld SK, Teichmann SA and Luscombe NM. A census of human transcription factors: function, expression and evolution. Nat Rev Genet 2009; 10: 252-263.
[46] Eulgem T, Rushton PJ, Robatzek S and Somssich IE. The wrky superfamily of plant transcription factors. Trends Plant Sci 2000; 5: 199-206.
[47] Ulasov AV, Rosenkranz AA and Sobolev AS. Transcription factors: time to deliver. J Control Release 2018; 269: 24-35.